ALMA MATER STUDIORUM
UNIVERSITÀ DI BOLOGNA

ARCHIVIO ISTITUZIONALE
DELLA RICERCA

Alma Mater Studiorum Università di Bologna
Archivio istituzionale della ricerca

Competitive sorption in CO2/CH4 separations: the case of HAB-6FDA polyimide and its TR derivative and a general analysis of its impact on the selectivity of glassy polymers at multicomponent conditions

This is the final peer-reviewed author's accepted manuscript (postprint) of the following publication:

Published Version:
Ricci E., Benedetti F.M., Dose M.E., De Angelis M.G., Freeman B.D., Paul D.R. (2020). Competitive sorption in CO2/CH4 separations: the case of HAB-6FDA polyimide and its TR derivative and a general analysis of its impact on the selectivity of glassy polymers at multicomponent conditions. JOURNAL OF MEMBRANE SCIENCE, 612(15 October 2020), 1-16 [10.1016/j.memsci.2020.118374].

Availability:
This version is available at: https://hdl.handle.net/11585/769515 since: 2023-11-24

Published:
DOI: http://doi.org/10.1016/j.memsci.2020.118374

Terms of use:

Some rights reserved. The terms and conditions for the reuse of this version of the manuscript are specified in the publishing policy. For all terms of use and more information see the publisher's website.

This item was downloaded from IRIS Università di Bologna (https://cris.unibo.it/).
When citing, please refer to the published version.

(Article begins on next page)

12 October 2024

This is the final peer-reviewed accepted manuscript of:

Eleonora Ricci, Francesco M. Benedetti, Michelle E. Dose, Maria Grazia De Angelis, Benny D. Freeman, Donald R. Paul, Competitive sorption in CO2/CH4 separations: the case of HAB-6FDA polyimide and its TR derivative and a general analysis of its impact on the selectivity of glassy polymers at multicomponent conditions, Journal of Membrane Science, Volume 612, 2020, 118374, ISSN 0376-7388

The final published version is available online at: **https://doi.org/10.1016/j.memsci.2020.118374**

Terms of use:

Some rights reserved. The terms and conditions for the reuse of this version of the manuscript are specified in the publishing policy. For all terms of use and more information see the publisher's website.

This item was downloaded from IRIS Università di Bologna (https://cris.unibo.it/)

When citing, please refer to the published version.

Journal Pre-proof

Competitive sorption in CO_2/CH_4 separations: the case of HAB-6FDA polyimide and its TR derivative and a general analysis of its impact on the selectivity of glassy polymers at multicomponent conditions

Eleonora Ricci[1], Francesco M. Benedetti[1,§], Michelle E. Dose[2], M. Grazia De Angelis[1,], Benny D. Freeman[2], Donald R. Paul[2]*

[1]Department of Civil, Chemical, Environmental and Materials Engineering, Alma Mater Studiorum – University of Bologna, Italy

[2]John J. McKetta Jr. Department of Chemical Engineering – The University of Texas at Austin, United States

[§]**Present address:** Department of Chemical Engineering – Massachusetts Institute of Technology, United States

***Corresponding author:**

Maria Grazia De Angelis

grazia.deangelis@unibo.it

Tel. +39 (0) 51 2060410

Fax +39 (0) 51 6347788

Journal Pre-proof

- CRediT author statement-

Eleonora Ricci: Methodology, Investigation, Formal Analysis, Software, Writing - Original Draft **Francesco M. Benedetti:** Methodology, Investigation, Formal Analysis**,** Writing - Original Draft **Michelle E. Dose:** Resources, Writing - Review and Editing **Maria Grazia De Angelis:** Conceptualization, Writing - Review and Editing, Supervision **Benny D. Freeman:** Writing - Review and Editing, Supervision **Donald R. Paul:** Writing - Review and Editing, Supervision

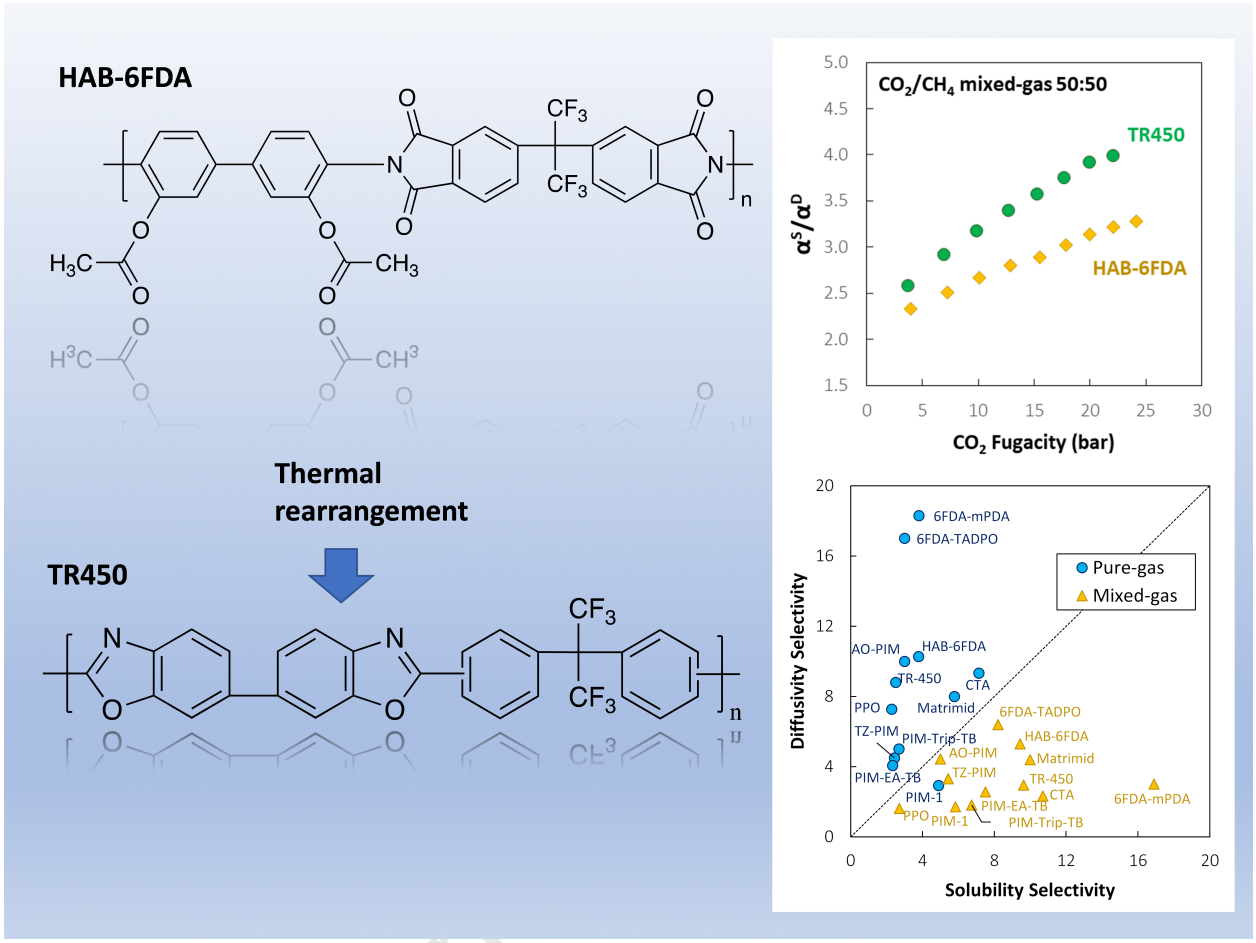
HAB-6FDA
Thermal rearrangement
TR450
CO2/CH4 mixed-gas 50:50
TR450
HAB-6FDA
αS/αD
CO2 Fugacity (bar)
Pure-gas
Mixed-gas
Diffusivity Selectivity
Solubility Selectivity
6FDA-mPDA
6FDA-TADPO
AO-PIM
HAB-6FDA
TR-450
CTA
PPO
Matrimid
TZ-PIM
PIM-Trip-TB
PIM-EA-TB
PIM-1

Journal Pre-proof

Competitive sorption in CO_2/CH_4 separations: the case of HAB-6FDA polyimide and its TR derivative and a general analysis of its impact on the selectivity of glassy polymers at multicomponent conditions

Eleonora Ricci[1], *Francesco M. Benedetti*[1,§], *Michelle E. Dose*[2], *M. Grazia De Angelis*[1,*], *Benny D. Freeman*[2], *Donald R. Paul*[2]

[1]Department of Civil, Chemical, Environmental and Materials Engineering, Alma Mater Studiorum – University of Bologna, Italy

[2]John J. McKetta Jr. Department of Chemical Engineering – The University of Texas at Austin, United States

[§]**Present address:** Department of Chemical Engineering – Massachusetts Institute of Technology, United States

***Corresponding author:**
Maria Grazia De Angelis
grazia.deangelis@unibo.it

Tel. +39 (0) 51 2060410
Fax +39 (0) 51 6347788

Journal Pre-proof

Journal Pre-proof

Abstract

CO_2 and CH_4 mixed-gas solubility was measured in 3,3'-dihydroxy-4,4'-diamino-biphenyl (HAB) 2,2'-bis-(3,4-dicarboxyphenyl) hexafluoropropane dianhydride (6FDA) polyimide and in its thermally rearranged (TR) derivative, TR450. Due to competitive sorption effects, the solubility of both species in mixed-gas conditions is lower than the corresponding pure-gas solubility at the same fugacity. CH_4 sorption is significantly affected by the presence of the second gas, while CO_2 behavior is hardly altered. Therefore, the multicomponent solubility-selectivity is higher than the ideal value calculated from pure-gas sorption data, and this has a positive impact on CO_2/CH_4 separation properties. The multicomponent solubility data were modelled with the Non-Equilibrium Lattice Fluid (NELF) model, using only pure component parameters and binary interaction parameters obtained from pure-gas sorption data available in the literature, with no parameters determined from the mixed-gas sorption data. Although it is easier to use, the multicomponent Dual Mode Sorption (DMS) model yielded less accurate predictions of mixed-gas sorption. Mixed-gas sorption experiments and modelling, coupled with mixed-gas permeation data, enabled a better fundamental understanding of the separation properties of these materials. Unlike the case for pure-gas experiments, where diffusivity contributes more to the overall ideal selectivity, competitive sorption is the main effect governing the permselectivity of these membrane materials at multicomponent conditions. A systematic comparison with literature data on mixed-gas CO_2/CH_4 sorption and permeability revealed these to be generalized trends, obeyed by materials of very different chemical constitution. This can inform on the criteria that make polymers performing better in multicomponent scenarios, with potential impact on the design and synthesis strategies of new materials.

Keywords: gas separation; mixed-gas sorption; TR polymers; solution-diffusion; NELF model.

Journal Pre-proof

1. Introduction

Membrane gas separation has been successfully employed industrially for more than forty years, with the first plants for air separation and CO_2 removal from natural gas dating to the 1980s [1]. Nowadays, membrane materials design is an active area of research [2-13] that aims to improve current applications, such as hydrogen recovery, air separation, and natural gas and biogas treatment. Moreover, if suitable materials are identified, the scope of the technology could be expanded to other potential separations, such as C_2 and C_3 alkane/alkene separation, CO_2 capture from flue gas or syngas streams, and separation of organic vapors [14–18], that are currently accomplished using techniques such as distillation, solvent absorption or pressure swing absorption.

However, despite an ongoing effort in synthesizing and characterizing countless new materials, traditional polymers (*e.g.*, cellulose acetate and polysulfone) remain prominent in industry, with few innovations having been adopted over the years. The very first reason listed by Baker *et al.* [1] for this failure of new materials to penetrate the market is that pure-gas measurements are poor predictors of membrane performance under realistic industrial conditions. Indeed, at the laboratory scale, screening tests for prospective membranes are seldom performed at relevant temperature and pressure ranges for the target application, or with mixture compositions representative of those in actual practice. Consequently, test results often inaccurately predict how the material will perform in real operating conditions.

Separation with dense polymeric materials is generally described by the solution-diffusion model [19], according to which two factors – *i.e.*, gas solubility and gas diffusivity – determine permeability and the permselectivity of the materials to various penetrants. By analyzing these factors separately, with pure- and mixed-gas measurements, we can understand at a more fundamental level which physical phenomena ultimately determine the performance of a material. For example, for CO_2/CH_4 separation, the permselectivity at mixed-gas conditions can be markedly different from the pure-gas permselectivity, sometimes for the better [20–22] and other times for the worse [14,23–26], whereas in other cases it remains almost unchanged [27,28]. CO_2/CH_4 mixed-gas sorption measurements in glassy polymers showed that, for both species, the solubility in multicomponent conditions is always lower than it is under pure-gas conditions at fixed partial pressure due to competitive sorption between CO_2 and CH_4. Depending on the mixture composition, however, the strength of the exclusion effect can vary and often influences one

gas more than the other. Nonetheless, because CO_2 is much more soluble than CH_4, its solubility is only weakly affected by the presence of methane over a wide range of mixture compositions, whereas the opposite happens to CH_4: its solubility is significantly lowered by the presence of even low levels of CO_2, often leading to a substantial increase in the CO_2/CH_4 solubility-selectivity. To date, this behavior has been documented in several glassy polymers: hexafluorodianhydride–3,3,4,4-tetraaminodiphenyl oxide polypyrrolone (6FDA-TADPO) [27], poly(1-trimethylsilyl-1-propyne) (PTMSP) [29], polybenzodioxane PIM-1 [30,31], tetrazole-modified PIM-1 (TZ-PIM) [32], 4,4'-(hexafluoroisopropylidene) diphthalic dianhydride-m-phenylenediamine (6FDA-mPDA) [28], and poly-Tröger's base ladder polymer of intrinsic microporosity PIM-Trip-TB [33]. Moreover, competitive sorption effects have also been reported for CO_2/CH_4 sorption in a rubbery polymer, polydimethylsiloxane (PDMS) [34], and in other systems, such as CO_2/C_2H_4 and CO_2/N_2O sorption in PMMA [35–37], CH_4/n-C_4H_{10} sorption in PTMSP [38] and PDMS [39], CO_2/C_2H_6 sorption in a cross-linked poly(ethylene oxide) copolymer [40].

By coupling multicomponent sorption and permeation measurements, multicomponent diffusivity-selectivity can be evaluated indirectly, by means of the solution-diffusion model, as detailed in section 3.1 of this study. The multicomponent diffusivity-selectivity thus calculated for various glassy polymers is lower than the corresponding pure-gas diffusivity-selectivity, and this phenomenon is attributed to the fact that CO_2 swells the polymer matrix, promoting faster diffusion of CH_4, which is not able to dilate the polymer to the same extent when permeating alone [32,41].

Recently, experimental techniques were reported for direct determination of gas diffusivity in multicomponent conditions. Garrido *et al.* [42] used a combination of ^{13}C NMR spectroscopy and pulsed-field gradient NMR to determine the solubility and diffusion coefficients of gas mixtures, including CO_2/CH_4, in poly(4,4-hexafluoroisopropylidene diphthalic anhydride-2,3,5,6-tetramethyl-1,4-phenylenediamine) (6FDA-TMPDA) polyimide. Fraga *et al.* [22] developed a time-lag technique to measure diffusivity in mixed-gas conditions, based on mass spectroscopy analysis of permeate composition during transient permeation, and they applied it to study the behavior of a CO_2/CH_4 mixture in PIM-EA-TB, an ethanoanthracene-based (EA) polymer of intrinsic microporosity (PIM) synthesized via the Tröger's base (TB) polymerization reaction [43]. In both cases, multicomponent diffusivity-selectivity values were lower than corresponding pure-gas values, supporting the theoretical predictions.

It is critical to separate the sorption and diffusion contributions to the overall permeation performance of a material. In this way, one can assess whether, in multicomponent permeation, separation properties (*e.g.*, permselectivity) are controlled by sorption or by diffusion. Moreover, such results, when compared with analogous pure-gas data, allow us to understand whether pure-gas data is or is not representative of mixed-gas permeation performance. Therefore, such results provide valuable insight for design of new materials.

In this study, the relative contributions of solubility-selectivity and diffusivity-selectivity to overall permeability selectivity are isolated by performing mixed-gas CO_2/CH_4 sorption tests and coupling them with mixed-gas permeability data from the literature. Lanč *et al.* [44] recently reported an analysis of gas solubility coefficients either determined directly from sorption experiments or obtained indirectly from permeability and diffusion coefficient measurements. They considered several high free volume glassy polymers, mostly polymers of intrinsic microporosity (PIMs). The authors identified a source of inaccuracy in the indirect determination of the solubility coefficient when it is obtained under the hypothesis of a linear concentration profile across the membrane, as assumed by time-lag analysis. This discrepancy can be mitigated, although not fully reconciled, if more realistic concentration profiles are calculated, using the thermodynamic version of Fick's law [45].

The materials considered in this study are chemically imidized HAB-6FDA polyimide, which will be referred to as HAB-6FDA for brevity, and its thermally rearranged (TR) analogue, referred to as TR450 [46]. Aromatic polyimides exhibit excellent thermal, mechanical and chemical stability [26,47] and have already found commercial application in CO_2/CH_4 membrane separations [15]. On average, these materials are characterized by low permeability and high ideal selectivity, owing to their high chain stiffness and low free volume, which enhances differences in the mobility of penetrants inside the polymer. However, if dianhydrides incorporating a spiro center are used, polyimides of intrinsic microporosity can be obtained (PIM-PI). In these materials, the use of kink units promotes less efficient chain packing, resulting in higher free-volume and, consequently, higher gas permeability accompanied by moderate permselectivities [48,49].

TR polymers [50–52] constitute another interesting class of materials for gas separation applications, comprising polybenzoxazoles (PBO) and polybenzothiazoles (PBT), which are characterized by excellent thermal and chemical stability. Because of their exceptional chemical resistance, they are insoluble in most solvents and, therefore, not processable and unsuitable for membrane fabrication. Nonetheless, Park *et al.* [50] circumvented this limitation by showing that, starting from aromatic polyimide precursors that were highly

soluble in common solvents, they could obtain insoluble PBO and PBT membranes through an irreversible molecular rearrangement process at high temperatures (350 – 450 °C). Since this viable processing route to obtain PBO and PBT films became available, these materials have received increasing attention for membrane separation applications [13,53–58]. They show higher permeability values with respect to the polyimide precursors while maintaining good selectivity, which make them interesting candidates for gas separation, especially for CO_2/CH_4 and CO_2/N_2 separations; for these gas pairs, these materials lie above the 2008 Robeson upper bound [59,60]. Positron annihilation lifetime spectroscopy (PALS) measurements and molecular modelling have revealed that, during the rearrangement process, a favorable free volume distribution for gas separation is created, which is described as hourglass-shaped. A large average cavity size, favoring high permeability, is coupled with a narrow cavity distribution and small bottlenecks connecting the cavities, which confer higher ideal selectivity compared to other materials with a similar fractional free volume [50,51,61,62]. The rigid backbone structure of PBOs, made up of interconnected heterocyclic rings that have very high rotational barriers, making the microstructure of the materials rather stable in regards to ageing and plasticization, as evidenced by low hysteresis in repeated pressurization-depressurization cycles [50,63–65]. This characteristic is critical when CO_2, water or other condensable species, such as heavy hydrocarbons, are present in the mixture to be separated.

The gas transport properties of HAB-6FDA and its TR derivatives have been extensively characterized: pure-gas sorption [46], pure-gas permeation [66] and mixed-gas permeation of CO_2 and CH_4 [20], also as a function of temperature [67], have been reported. In this study, characterization of these materials was expanded by performing mixed-gas CO_2/CH_4 sorption experiments.

Because mixed-gas sorption tests are significantly more sensitive and time-consuming than pure-gas tests, there is a great potential advantage in using modelling tools to predict mixed-gas behavior using only pure-gas information. If model predictions are shown to be reliable, meaningful information about multicomponent behavior could be obtained directly from the pure-gas data already extensively available in the literature.

Mixed-gas sorption calculations can be performed using the well-established Dual Mode Sorption (DMS) model [68–77], which was extended and applied to multicomponent mixtures by Koros *et al.* [78–80]. Alternatively, one can use thermodynamics-based models to predict sorption equilibria in glassy polymers. The Non-Equilibrium Thermodynamics for Glassy Polymers approach (NET-GP) [81–85] provides an extension of the Equations of

State (EoS) approach to nonequilibrium materials and has been successfully applied to calculate gas and vapor sorption in glassy polymers [85–90]. Both the multicomponent DMS and the NET-GP approaches will be described in a following section; it is significant to note that they can perform mixed-gas sorption calculations predictively, since only pure-gas sorption data are needed to parameterize them.

In this work, mixed-gas CO_2/CH_4 sorption isotherms in HAB-6FDA and its TR450 variant were predicted using pure-gas sorption isotherms as input, employing both the DMS model and the NET-GP approach. The results of the calculations and the accuracy of the models were validated through direct comparison with measured experimental data.

Journal Pre-proof

2. Materials and Methods

2.1. Polymer synthesis and film casting

HAB-6FDA polyimide (**Figure 1a**) was synthesized from 3,3'-dihydroxy-4,4'-diamino-biphenyl (HAB) and 2,2'-bis- (3,4-dicarboxyphenyl) hexafluoropropane dianhydride (6FDA) by a two-step polycondensation method with chemical imidization, using a method that was previously reported [46] and here briefly recalled. Prior to use, HAB (> 99 %, *ChrisKev*) was dried at 50 °C under vacuum for 24 h. 6FDA (99%, *Sigma Aldrich*) was dried in a vacuum oven for 6 h at 200 °C at -10 inHg, then cooled to 120 °C and dried under full vacuum for 24 h. After flame drying all glassware to minimize exposure to water, 20 mmol of HAB was added to 80 mL of N-methyl-2-pyrrolidone (NMP) (anhydrous, 99.5%, *Sigma Aldrich*) and stirred with a mechanical stirrer until the diamine dissolved completely. After placing the reaction flask in an ice bath, 20 mmol of 6FDA was slowly added to the mixture, allowing each addition to dissolve prior to the next addition. An additional 10 mL of NMP was added to the flask to bring the mixture to 15 wt% solids. The resulting mixture was stirred for roughly 12 h, allowing the solution to gradually return to room temperature. The resulting poly(amic acid) was imidized using standard chemical imidization techniques [46,91,92]. To the reaction flask, 160 mmol of pyridine (anhydrous, 99.8%, *Sigma Aldrich*) and 160 mmol of acetic anhydride (ACS Reagent Grade, >98.0%, *Sigma Aldrich*) were added, along with additional NMP to bring the mixture to 5 wt% solids. Imidization was allowed to proceed at room temperature for 24 h, while stirring. The resulting polyimide was precipitated in methanol (solvent grade, *Fisher Scientific*), and the solids were separated from the reaction mixture by vacuum filtration. To remove any residual solvent, the polyimide powder was soaked in methanol for 24 h, followed by vacuum filtration, and it was dried under full vacuum for 24 h at 120 °C and then 48 h at 200 °C.

Polymer films were cast from N,N-dimethylacetamide (DMAc) solutions of approximately 5 wt% solids. Solutions were filtered through a 5 μm polytetrafluoroethylene filter and cast onto a flat glass plate with a glass ring attached. Films were dried in a vacuum oven at 80 °C overnight at -10 inHg. As the solvent evaporated, additional vacuum was pulled to maintain a partial vacuum of -10 inHg. After the bulk of the solvent was removed, the resulting film was dried at 200 °C under vacuum overnight to remove residual DMAc. Thermogravimetric analysis confirmed that this protocol ensures total removal of the solvent [46].

2.2. Thermal Rearrangement

The rearrangement reaction is typically performed at temperatures from 350 to 450 °C [46]. The mass loss during the process is used to estimate the conversion of the polyimide precursor to the final PBO TR structure (**Figure 1b**) because, in the absence of significant thermal degradation, all mass loss should be due to thermal rearrangement. Eq. (1) was used to estimate the percent conversion of the polyimide precursor to TR polymer, which was about 71% for the material used in this study:

$$\%\ \text{Conversion} = \frac{\text{Actual mass loss}}{\text{Theoretical mass loss}} \times 100 \qquad \text{Eq. (1)}$$

Thermal rearrangement was performed by first placing the polyimide films between ceramic plates to prevent curling. The ceramic plates were then placed in a tube furnace and a nitrogen (*Airgas*, 99.999%) flowrate of 900 mL/min was used to create an inert environment during the thermal treatment. The samples were then heated to 300 °C, using a ramp rate of 5 °C/min, and held at 300 °C for 1 h to ensure complete imidization. Then, temperature was increased at 5 °C/min to the target thermal rearrangement temperature (450 °C), where the sample was held for the desired amount of time (30 minutes). The furnace was then cooled to ambient conditions at a rate no greater than 10 °C/min. After treatment, the films were not cracked or curled and were suitable for subsequent transport and characterization. This heating protocol was used to expose the samples to thermal histories similar to those reported in previous studies of TR polymers, as it ensures minimal thermal degradation and yields percent conversions comparable to those of previous studies [20,46,50,51,66]. The properties of the samples and the amount of each polymer used for the sorption tests are summarized in **Table 1**. Of note, the TR450 sample was obtained from a fresh sample of HAB-6FDA that was not previously tested at the pressure decay.

(a) HAB-6FDA

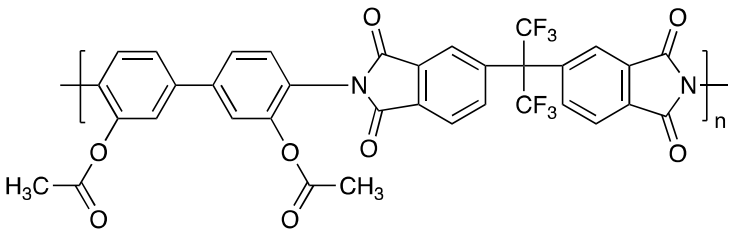

Journal Pre-proof

(b) TR450

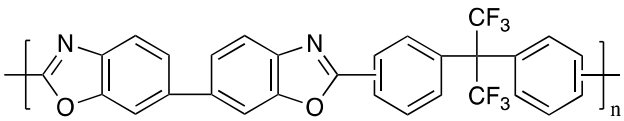

Figure 1*: Chemical structures of (a) HAB-6FDA, and (b) TR450.*

Table 1. *Properties of HAB-6FDA and TR450 samples used for pure- and mixed-gas sorption test.*

	Thickness (μm)	**Mass (g)**	**Density (g/cm^3)** [93]	**FFV (%)** [66]	**Conversion (%)**
HAB-6FDA	55 ± 4	0.342	1.407 ± 0.009	15.0	/
TR450	43 ± 1	0.351	1.340 ± 0.010	19.6	70.8

2.3. Mixed-Gas Sorption Tests

Using an in-house built apparatus already described in detail [29,30], we performed mixed-gas sorption tests for a CO_2/CH_4 gas mixture at an equilibrium composition of about 30 mol% CO_2 at different total equilibrium pressures. The system is shown schematically in **Figure 2** and consists of a pressure decay device coupled to a gas chromatograph (*Varian Inc. – CP-4900 Micro GC*). The apparatus is submersed in a water bath to maintain temperature control and can function over a wide range of pressures (0-35 bar), temperatures (25-65 °C), and compositions (0-100 mol% CO_2). A *Honeywell-Super TJE* pressure transducer (PT01) with a full-scale range of 500 psia was used to measure the pressure. To stabilize the pressure reading with respect to temperature fluctuations, that part of the pressure transducer not immersed in the water bath was further insulated using a heating coil in which the fluid of the bath is continuously recirculated. All tests were performed at 35 °C.

The measurement protocol adopted for mixed-gas tests with this apparatus was optimized to maximize the flexibility of the equipment. It was reported in greater detail elsewhere [29] and is recalled here briefly for the reader's convenience. Initially, the loading pressures of the two gases need to be estimated, in order to obtain the desired composition (in the present case, 30 mol% CO_2) of the final gas mixture in equilibrium with the sample. This is accomplished by using pure-gas sorption isotherms to parameterize the NELF model (as detailed in the next section) and then employing the model to predict the gas concentration sorbed inside the polymer in pure- as well as in mixed-gas conditions. With this information, mass balances can be solved to calculate the loading pressures of the two gases. The first step in a mixed-gas equilibrium point measurement requires pressurizing the pre-chamber with the more condensable gas (CO_2) after keeping the sample under vacuum overnight. The gas is then

expanded into the sample chamber. Once a constant pressure is reached, V05 (see **Figure 2**) is closed and the pre-chamber is evacuated. This first part of the experiment is a pure-gas pressure decay sorption experiment step, allowing us to collect pure-gas CO_2-sorption information while also performing mixed-gas experiments. Subsequently, the less condensable gas, CH_4, is loaded in the pre-chamber at the desired pressure, and V05 is opened to allow the two gases to mix. When a constant pressure is reached, the polymer sample is isolated (V05 is closed), and the gas mixture, now at equilibrium pressure and composition, is expanded from the pre-chamber into the backup volume, used as a reservoir from which samples of gas are collected to measure the gas composition with a gas chromatograph (GC). These measurements provide the necessary information to calculate, via mass balances, the amount of each gas sorbed by the sample. Because of the high sensitivity of the final sorption values to the GC results, the GC test is repeated at least 10 times to minimize the experimental uncertainty in the gas phase composition. High repeatability in the composition measurement was verified, with values for standard deviations of the mean below 0.2%, an acceptable threshold for these tests.

The order in which the gases are fed to the apparatus is important because of their different conditioning effects on the membrane structure. CO_2, being predominantly responsible for any polymer dilation, is the first gas to which the polymer is exposed. In this way, when the second gas, CH_4, is loaded into the system, the polymer density is already comparable to the relaxation conditions that would result if the membrane were exposed directly and continuously to a mixture at 30 mol% of CO_2. The amount of CH_4 absorbed is thus closer to that of a real-world membrane separation apparatus. Operating the other way around, pure CH_4 would not cause the same extent of polymer swelling, and the overall amount of CH_4 absorbed would likely be underestimated. In mixed-gas tests, vacuum is pulled after each equilibration stage, and therefore a sorption isotherm is obtained through a series of “integral” steps, in which the equilibrium pressure is progressively increased. The loading pressures of both gases are estimated to obtain the same equilibrium mixture composition (*i.e.*, 30 mol% in this case) for each pressure point in the sorption isotherm. Conversely, “differential” steps are usually performed to obtain a pure-gas sorption isotherm. The procedure used to perform “differential” steps differs from that used to perform “integral” ones because each point of a sorption isotherm taken in a “differential” experiment is obtained by adding gas to increase the pressure in the polymer chamber already at equilibrium with the gas from the previous point. Pure gas sorption isotherms of CO_2 and CH_4 in HAB-6FDA and of CH_4 in TR450 were measured with the differential method, while

pure CO_2 sorption in TR450 was measured with the integral method, during the first step of each mixed-gas sorption test, as described previously.

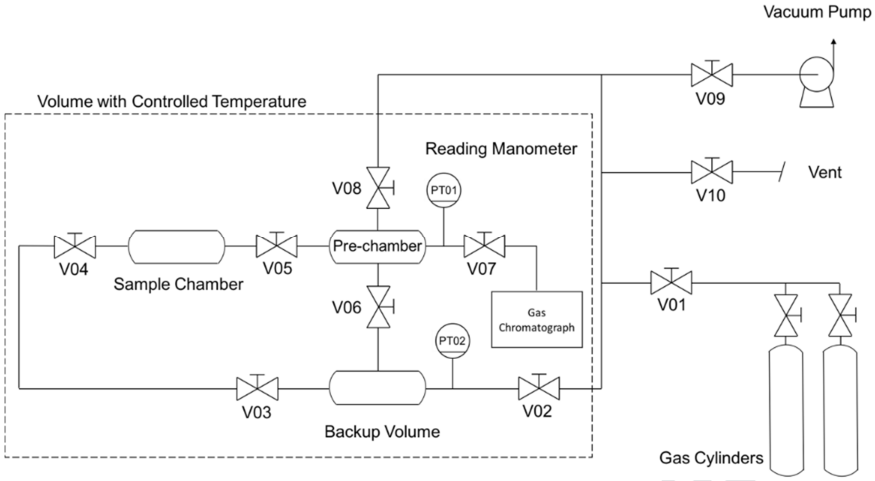

Figure 2. *Schematics of the pressure decay apparatus used to measure mixed-gas sorption isotherms.*

Journal Pre-proof

3. Theoretical Background

3.1. Solution-Diffusion Model

The transport of small molecules in dense polymeric membranes is described by the solution-diffusion model [19]. In this model, the permeability (P_i), which is defined as the steady-state flux of species *i* multiplied by membrane thickness and divided by the driving force (i.e., fugacity difference across the membrane), can be expressed as the product of the solubility (S_i) and diffusion coefficients (D_i) of species *i*, provided that the penetrant diffuses through the material following Fick's Law and that there is negligible pressure on the permeate side:

$$P_i = S_i D_i \qquad \text{Eq. (2)}$$

In this model, the selectivity of the polymer (permselectivity), which is equal to the ratio between the permeability coefficients of the two gases, contains a solubility-selectivity and a diffusivity-selectivity factor:

$$\alpha_{i,j} = \frac{P_i}{P_j} = \frac{S_i}{S_j}\frac{D_i}{D_j} = \alpha_{i,j}^S \alpha_{i,j}^D \qquad \text{Eq. (3)}$$

Our work is focused on sorption measurements and modelling. To calculate the solubility-selectivity, the following relation was used:

$$\alpha_{i,j}^S = \frac{S_i}{S_j} = \frac{c_i/f_i}{c_j/f_j} \qquad \text{Eq. (4)}$$

where c_i is the concentration, and f_i is the fugacity of each gas. If the concentrations used in Eq. (4) were measured in a mixed-gas experiment, the multicomponent solubility-selectivity would be obtained. If these values are not available and pure-gas concentrations are used instead, the expression remains the same, but the so-called *ideal* solubility-selectivity is calculated. The fugacity of the gases at various pressures was calculated using the Peng-Robinson equation of state [94]; the binary parameter k_{CO_2/CH_4} = 0.09 [95] was used for the mixed-gas case at all compositions.

3.2. Dual Mode Sorption Model

The most widely used model to represent gas sorption isotherms in glassy polymers is the Dual Mode Sorption (DMS) model [68–77]. According to this model, two different gas populations can be recognized inside a glassy polymer, one dissolved in the dense portion of

the material, whose behavior can be described by Henry's law, and one saturating the nonequilibrium excess free volume of the polymer, described by a Langmuir isotherm, typically used to describe gas sorption in porous materials. The total concentration of sorbed gas, as a function of gas fugacity, can be expressed as a sum of these two contributions:

$$c_i = k_{D,i} f_i + \frac{C'_{H,i} b_i f_i}{1 + b_i f_i} \qquad \text{Eq. (5)}$$

The parameter $k_{D,i}$ is Henry's law constant, b_i is the Langmuir affinity constant, and $C'_{H,i}$ is the Langmuir capacity constant. For every gas-polymer pair, these three parameters are estimated via a nonlinear least-square best fit of sorption data.

The extension of this model [78,79] to multicomponent sorption is based on the argument that the presence of a second penetrant *j* will not affect the capability of the first penetrant *i* to sorb in the Henry's law mode. However, the various penetrants will compete to occupy the unrelaxed free volume of the polymer and, consequently, the sorbed gas concentration in the Langmuir mode is expected to decrease with respect to the pure-gas case for both penetrants. This model hypothesizes that the amount of unrelaxed free volume is fixed and limited. Under the further hypothesis that the affinity parameter, b, Henry's constant, k_D, and the molar density of a component sorbed inside the Langmuir sites are independent of the presence of other penetrants, the expression for the concentration of component *i* in the presence of a second component *j* is as follows:

$$c_i = k_{D,i} f_i + \frac{C'_{H,i} b_i f_i}{1 + b_i f_i + b_j f_j} \qquad \text{Eq. (6)}$$

In this expression, the characteristic gas-polymer parameters of the model are identical to those obtained from the best fit of pure-gas isotherms calculated using Eq. (5). Once these parameters are determined from the pure-gas data, they can be used to predict the concentration of each gas at mixed-gas conditions, at any composition of interest, via Eq. (6).

3.3. Nonequilibrium Lattice Fluid Model

The Non-Equilibrium Thermodynamics for Glassy Polymers (NET-GP) approach [81–85] is a thermodynamics-based framework that provides an extension of Equation of State (EoS) theories to nonequilibrium materials, like glassy polymers. Therefore, it is suitable for calculating the solubility of low molecular weight species in glassy polymers. In the NET-GP approach, the state of the system is described by the same set of state variables as in equilibrium thermodynamics models, *i.e.* temperature, pressure and composition. However,

in addition, the actual nonequilibrium density of the glassy polymer, ρ_{pol}, which is responsible for its departure from equilibrium, is used as an internal state variable and accounts for all effects of thermal history and formation of the polymer. This approach provides expressions for the nonequilibrium chemical potential of an EoS of choice to be used in phase-equilibrium calculations that yield sorption isotherms:

$$\mu_i^{NE(pol)}\left(T, p, \Omega, \rho_{pol}\right) = \mu_i^{Eq(gas)}(T, p, y) \qquad \text{Eq. (7)}$$

where T is the temperature and p the pressure of the system, Ω is the composition vector of the polymer phase, y is the composition vector of the gas phase, ρ_{pol} is the nonequilibrium density of the polymer phase, $\mu_i^{NE(pol)}$ is the chemical potential of species i in the polymer phase, and $\mu_i^{Eq(gas)}$ is the chemical potential of species i in the gas phase.

Specifically, the Non-Equilibrium Lattice Fluid (NELF) model [81–83], which is the extension of the Sanchez-Lacombe (SL) EoS [96–98] to the nonequilibrium state of glassy polymers by means of the NET-GP theory, was used in this work to calculate sorption equilibria. In the lattice fluid representation, matter is seen as a lattice whose cells can be empty or occupied by sections of a molecule, and expressions for the energy and entropy of the system are obtained through statistical thermodynamics arguments. The characteristic pure-component parameters used in those expressions are: the molar volume of a lattice cell of component i (v_i^*), number of lattice cells occupied by a molecule of component i (r_i), and the non-bonded interaction energy between two cells occupied by component i (ε_i^*). Alternatively, the characteristic temperature (T_i^*), pressure (p_i^*) and density (ρ_i^*) can be used. Their relationships with v_i^*, r_i and ε_i^* are given in **Table S1** of the SI file, alongside the definitions of all other pure-component parameters and reduced variables as well as mixing rules. Pure-component parameters from the literature for all components used in this work are summarized in **Table 3**.

The expression for the chemical potential of the SL model, to be used in Eq. (7), is given below.

$$\frac{\mu_i}{RT} = ln(\tilde{\rho}\phi_i) - ln(1-\tilde{\rho})\left[r_i^0 + \frac{r_i - r_i^0}{\tilde{\rho}}\right] - r_i - \tilde{\rho}\frac{r_i^0 v_i^*}{RT}\left[p_i^* + \sum_{j=1}^{N}\phi_i\left(p_j^* - \Delta p_{i,j}^*\right)\right] + 1 \qquad \text{Eq. (8)}$$

The term $\Delta p_{i,j}^*$ contains a binary interaction parameter, k_{ij}, which measures the departure of polymer-penetrant interactions from the geometric mixing rule predicted by Hildebrand's regular solution theory [99]. This parameter is obtained for each polymer-penetrant pair by

fitting pure-gas sorption isotherms in the low-pressure range. For the gas phase, which is an equilibrium phase, the density value used in Eq. (8) to calculate $\mu_i^{Eq(gas)}$ is obtained by solving the SL EoS (Eq. (9)) for the density:

$$\tilde{\rho} = 1 - \exp\left[-\frac{\tilde{\rho}^2}{\tilde{T}} - \frac{\tilde{p}}{\tilde{T}} - \tilde{\rho}\left(1 - \sum_i^N \frac{\phi_i}{r_i}\right)\right] \qquad \text{Eq. (9)}$$

On the other hand, for the calculation of $\mu_i^{NE(pol)}$ using Eq. (8), the density value cannot be obtained by solving the EoS, due to the nonequilibrium state of the polymer phase. In fact, the NET-GP approach requires *as input* the experimental value of the polymer density at each pressure point used in the computation of the sorption isotherm. Especially at high pressure, and when swelling gases like CO_2 are present, experimental dilation measurements are necessary. However, in the absence of such data, a linear relation between the polymer specific volume and the partial pressure of the penetrants can be assumed:

$$\frac{1}{\rho_{pol}} = \frac{1}{\rho_{pol}^0}\left(1 + \sum_{i=1}^{N_p} k_{sw,i} p_i\right) \qquad \text{Eq. (10)}$$

where ρ_{pol}^0 is the mass density of the dry polymer, N_p is the number of gaseous species in the mixture, p_i is the partial pressure of each gas in the gas phase, $k_{sw,i}$ is an adjustable swelling coefficient, and ρ_{pol} is the mass density of the dilated polymer. For each gas, the value of $k_{sw,i}$ can be obtained by fitting the pure-gas sorption isotherm in the high-pressure range, after the appropriate value of k_{ij} is obtained. Linear volumetric dilation with increasing gas pressure was observed experimentally during sorption of light gases in glassy polymers [100,101]. In some instances, however, a concave trend with pressure was also documented, curving either downward [102] or upward [103], with higher deviations from linearity at high pressure. However, in the absence of indications for the specific case at hand, and since partial pressures of CO_2 lower than 10 bar are used in the mixed-gas tests, a linear relation was adopted. This assumption yields good results in NELF model calculations of sorption of light gases in a variety of glassy polymers [85].

Journal Pre-proof

4. Results and Discussion

4.1. Experimental: Sorption Isotherms

Pure CH_4 sorption in HAB-6FDA was measured at 35 °C using the differential method, followed by pure CO_2 sorption measurement at the same temperature. For TR450, the pure CH_4 sorption isotherm was also measured first, using the differential method, while pure CO_2 sorption was obtained subsequently in the course of the mixed-gas test, as described previously. The comparison with pure CO_2 and CH_4 sorption isotherms from the literature [46,67] shows good agreement and is reported in **Figure S1** of the Supplementary Information file. In addition, diffusion coefficients of CO_2 and CH_4 in HAB-6FDA were calculated from analysis of sorption kinetics, and the results compared favorably with those obtained by using the time-lag method of Sanders *et al.* [66]. Pure-gas diffusion coefficients as a function of gas concentration are shown in the SI file, **Figure S2**, alongside the calculation procedure.

Subsequently, the mixed-gas sorption test was performed. **Figure 3** shows the experimental sorption data for a CO_2/CH_4 mixture in HAB-6FDA and TR450 at 35 °C. The average final composition of the gas mixture in equilibrium with the polymer was 28.9 ± 0.3 mol% CO_2 in the case of HAB-6FDA and 29.5 ± 0.2 mol% CO_2 in the case of TR450. Standard deviations were calculated using the law of propagation of unbiased errors, considering the uncertainties in pressure readings, volume calibration and gas phase composition analysis [104].

By comparing the mixed-gas result with the corresponding pure-gas sorption isotherms, it is possible to recognize, for both materials, the typical behavior observed for multicomponent sorption in glassy polymers [29–32]: the presence of around 70 mol% CH_4 has little effect on CO_2 sorption, while CH_4 is markedly affected by the presence of CO_2. In the case of HAB-6FDA, CH_4 experiences, on average, a 53% concentration decrease due to the presence of CO_2, while in the case of TR450, the decrease averages 51%, with respect to the pure-gas values at the same fugacity. For comparison, the average CO_2 sorbed concentration decrease is 4% in HAB-6FDA and 12% in TR450. These results highlight the competitive nature of multicomponent sorption in glassy polymers, with the less condensable gas being more strongly excluded from the polymer, even though it is the most abundant in the gas phase.

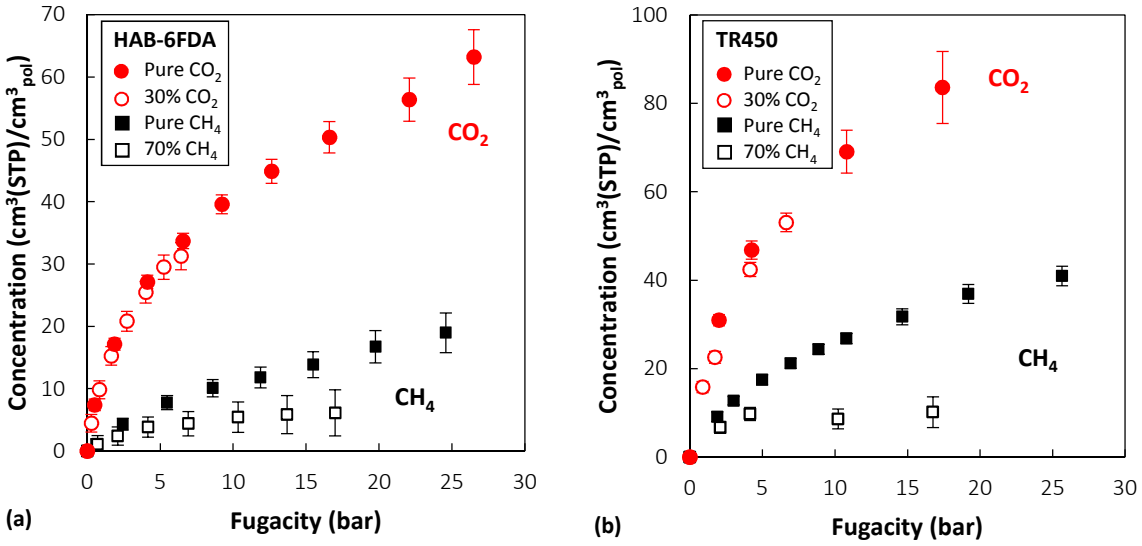

Figure 3. *Empty symbols: Mixed-gas sorption isotherms of CO_2 (red) and CH_4 (black) at 35 °C (~30 mol% CO_2 composition) in HAB-6FDA (a) and TR450 (b). Filled symbols: pure-gas CO_2 (red) and CH_4 (black) sorption isotherms.*

4.2. Modelling

4.2.1. Pure- and Mixed-gas Sorption Isotherms

Pure-gas CO_2 and CH_4 sorption isotherms at 35 °C in HAB-6FDA and TR450 were fit to the Dual Mode Sorption model using the fugacity-based relation in Eq. (5). The DMS model parameters are sensitive to, among other factors, the parameter estimation methodology [20,105–107]. Therefore, four different parameterization routes were examined. The different tests are described in detail in the Supplementary Information file and involved minimizing either the concentration or the solubility squared differences, and weighting or not weighting the squared differences with the inverse squared experimental errors [104]. The parameters obtained for CO_2 and CH_4 in both materials are summarized for each minimization method in **Table S2** of the SI file. A comparison of the pure- and mixed-gas sorption representation yielded by each parameter set is presented in **Figure S3** of the SI file. As expected, different parameter sets were obtained in each case, yielding predictions of varying accuracy for the mixed-gas case. In the case of HAB-6FDA, a very good representation of mixed-gas data was given by the parameter set obtained by minimizing the error-weighted solubility squared differences, even though this was accompanied by a less accurate pure CO_2 sorption representation, especially at high pressure, compared to the other cases. On the other hand, in the case of TR450, the parameters obtained by minimizing the unweighted concentration differences yielded the best results. The best parameter set for each of these best cases was selected and is recorded in **Table 2**. The pure-gas and mixed-gas sorption isotherms of a 30 mol% CO_2 mixture calculated with Eq. (6) are shown in **Figure 4**.

Table 2. *DMS model fugacity-based parameters for CO_2 and CH_4 sorption in HAB-6FDA and TR-450 at 35 °C.*

	Gas	k_D $\left(\frac{cm^3_{STP}}{cm^3_{pol}bar}\right)$	C'_H $\left(\frac{cm^3_{STP}}{cm^3_{pol}}\right)$	b (bar^{-1})
HAB-6FDA	**CO_2**	1.678	26.07	0.659
	CH_4	0.015	32.00	0.051
TR450	**CO_2**	1.852	57.95	0.470
	CH_4	0.812	26.01	0.215

Pure-gas sorption of several gases at different temperatures in HAB-6FDA and its TR variants was successfully modelled by Galizia *et al.* [93] using the NELF model. In their work, pure component parameters of the Sanchez-Lacombe EoS for HAB-6FDA and TR450 were obtained, as well as the binary interaction parameters and swelling coefficients for CO_2 and CH_4. Here, we used pure component parameter sets from the literature (reported in **Table 3**) to model our measured pure-gas sorption isotherms, in order to optimize the values of the adjustable parameters, k_{ij} and k_{sw}. The values obtained are reported in

Table 4.

Moreover, mixed-gas sorption calculations require the use of a binary interaction parameter for the gas pair. The value of the CO_2/CH_4 binary interaction parameter was optimized by fitting the CO_2/CH_4 pressure-volume-temperature-composition curves reported by Liu et al. [108] to the Sanchez-Lacombe EoS. The details of the calculation are reported in the SI file. A value of –0.03 was obtained, which was used in all mixed-gas sorption calculations with the NELF model. The effect of this parameter on the results is discussed in more detail below.

Table 3. *Pure component parameters for the Sanchez-Lacombe EoS of the gases and polymers considered in this study.*

	$T^*(K)$	$p^*\ (MPa)$	$\rho^*\ (g/cm^3)$	Ref.
HAB-6FDA	720	481.1	1.609	[93]
TR450	930	446.9	1.528	[93]
CO_2	300	630	1.515	[81]
CH_4	215	250	0.500	[83]

Journal Pre-proof

Table 4. *Binary interaction parameters and swelling coefficients used in mixed-gas sorption calculations with the NELF model at 35 °C.*

	k_{ij}	k_{sw} (MPa^{-1})
HAB-6FDA/CO_2	-0.025	0.007
HAB-6FDA/CH_4	0.052	0
TR450/CO_2	-0.085	0.023
TR450/CH_4	-0.037	0
CO_2/CH_4	-0.03	/

For comparison, the results of mixed-gas sorption calculations with the NELF model are presented in **Figure 4** alongside those obtained with the DMS model and the experimental measurements. Note that neither model requires additional parameters to take into account the mixed-gas effects in the ternary (i.e., polymer plus two different gases) system, and all the system-specific parameters come from the best fit of pure-gas sorption data. This makes these models potentially powerful tools, given that in recent decades pure-gas sorption has been characterized for a wide variety of polymer materials and that, for most of them, NELF and DMS parameters have been already reported in the literature or can be readily obtained.

As can be observed, both models qualitatively capture the competitive nature of the multicomponent sorption, predicting a reduction in the solubility of both gases in both materials. Quantitative agreement with the data, however, is markedly different among the various cases. For CO_2 sorption in HAB-6FDA, the results of the two models for the mixed-gas case are almost indistinguishable, with an average relative deviation of 6% from the experimental data in the case of NELF and 7% in the case of the DMS model. For CH_4 sorption in the same material, the DMS model prediction has an average 19% relative deviation from the data, while that of the NELF model is 8%. In the case of TR450, the DMS model accuracy (23% average deviation for CO_2, 100% for CH_4) is significantly lower than that of the NELF model (14% average deviation for CO_2, 25% for CH_4). The average experimental standard deviations offer a frame of reference for evaluating the accuracy of the modelling results: 12% and 63% in the case of CO_2 and CH_4 mixed-gas sorption in HAB-6FDA, while in the case of TR450 they are 5% and 24%, respectively. The average relative deviations obtained with the two models and the average confidence intervals are compared in **Figure S5** in the SI file.

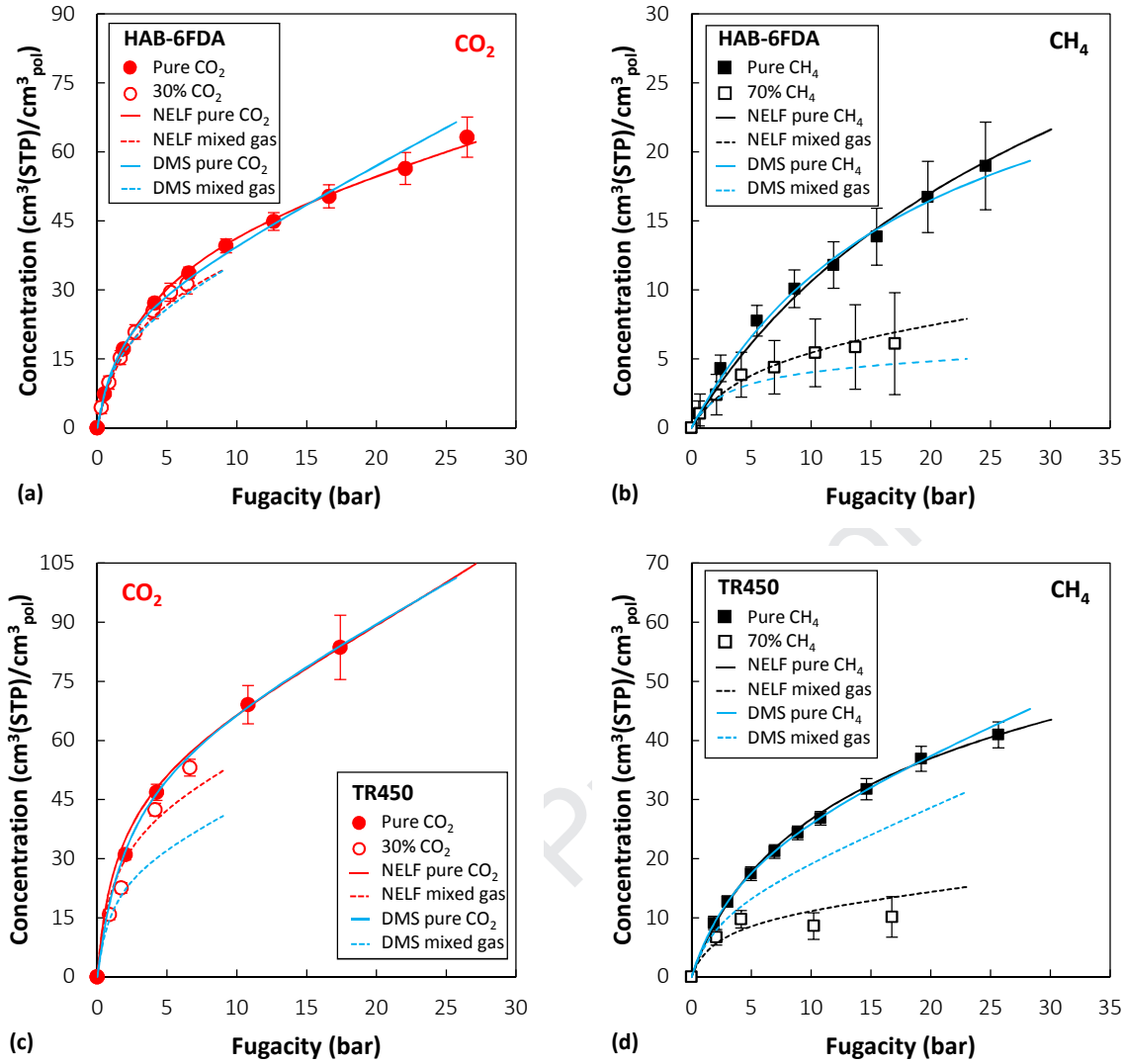

Figure 4. *Experimental data of pure- and mixed-gas (30 mol% CO_2) sorption isotherms at 35 °C of CO_2 (red) and CH_4 (black) in HAB-6FDA, (a) and (b) respectively, and TR450, (c) and (d) respectively, together with mixed-gas predictions obtained with the NELF model (dashed lines) and the multicomponent Dual Mode Sorption model (blue dot-dash lines).*

A potential source of variability in the NELF model calculation comes from the uncertainty in dry polymer density measurements. To test the robustness of the model with respect to this factor, the entire density error bar of HAB-6FDA and TR450 was covered to evaluate the effect of this quantity on mixed-gas sorption calculations. The effect of density variation on the values of the adjustable parameters is reported in **Table S5** in the SI, and the results are compared in **Figure S6** in the SI. Remarkably, the results show limited variability: at the extremes of the density error bar, the average relative deviations for CO_2 and CH_4 sorption in HAB-6FDA are 0.7% and 1.6%, respectively, while in the case of TR450, it is 0.9% for CO_2 and 3.8% for CH_4. Therefore, a small perturbation in the initial density value is compensated for by a variation of the adjustable coefficients, yielding consistent

multicomponent results, when the same pure-gas representation is obtained with a different parameter set.

In general, the NELF model yielded mixed-gas sorption results of more consistent accuracy, but this does not result from the use of a larger number of parameters. Indeed, the NELF model requires just 2 adjustable parameters for each gas, k_{ij} and k_{sw}, whereas the DMS model needs 3 adjustable parameters for each gas, k_D, b and C'_H. Moreover, the best DMS parameters were chosen, among the different sets obtained, by comparison with the experimental data. Regrettably, the best performing parameters were not found by following the same optimization routine for the two materials, which keeps this approach from being generalizable. Therefore, in the absence of experimental data for validation, it is not possible to anticipate which case would yield the best mixed-gas sorption prediction. As can be seen in **Figure S3**, for HAB-6FDA the discrepancies among the different cases would be extremely high.

Explanations for the deviation of the multicomponent DMS predictions from the experimental data were identified originally by Koros [78] in the possible presence of non-negligible penetrant-penetrant specific interactions or as a consequence of swelling and plasticization effects, not accounted for in the model, that would make the parameters concentration-dependent. The effect of neglecting specific penetrant-penetrant interactions can be evaluated in the NELF calculation, by setting the CO_2/CH_4 binary interaction parameter equal to zero. As shown in **Figure S7** in the SI, this had a negligible effect on the mixed-gas sorption results, both for CO_2 and CH_4 in HAB-6FDA and TR450, with average relative deviations from 0.15% to 1.2% between calculations made with $k_{ij} = -0.03$ or $k_{ij} = 0$. These results confirm the assumptions made in previous studies that used the NET-GP theory to calculate mixed-gas sorption calculation in glassy polymers [109]. Thus, penetrant-penetrant specific interactions are not believed to be a plausible explanation for the discrepancies that have emerged with the use of the DMS model. On the other hand, swelling is explicitly accounted for in the NELF model, unlike the DMS model. A sensitivity analysis of multicomponent DMS model calculations [110] showed that poor results in mixed-gas predictions can be ascribed to parametrization issues. Due to the strong coupling between parameters C'_H and b, several different parameter sets can be found that provide equally satisfactory representations of the pure-gas sorption isotherms, within experimental error [110]. But even though these different parameter sets gave equivalent representations of pure-gas data, their prediction of multicomponent sorption can be either really accurate or really poor. Therefore, in the absence of experimental data to validate the calculated results,

their accuracy cannot be assumed. Gleason *et al.* [20] reported similar issues in their analysis of Dual Mode parameters for mixed-gas permeation of CO_2/CH_4 in HAB-6FDA and TR-PBOs and so resolved to include the mixed-gas data in the parametrization. Although a better representation of the mixed gas data was achieved, this procedure is clearly not predictive.

Stevens *et al.* [67] reported DMS model parameters for CO_2 and CH_4 sorption in HAB-6FDA and TR450. In their work, the parameters were obtained using data sets for 3 gases (CO_2, CH_4, N_2) and at 5 temperatures simultaneously in the fitting procedure. Moreover, a temperature dependence and a relation with the critical temperature of the penetrants were imposed to further constrain the parameter values. This additional information was not used to determine our DMS parameters reported in **Table 2**.

The parameters obtained by Stevens *et al.* [67] are reported in **Table S3** for ease of comparison. They differ from those obtained in this work, as expected, since a different experimental data set and a different parametrization route were employed in their estimation. This DMS parameter set yielded a more accurate prediction in the multicomponent case (**Figure S4** of the supplementary information file), in the case of both HAB-6FDA and TR450. Especially for the TR450 case, this is striking, considering the limited difference in pure-gas sorption data representation yielded by the two parameter sets. However, especially for CO_2, a less faithful representation of the pure-gas data emerged, particularly in the high-pressure range. The higher reliability of a DMS parameter set optimized over a larger data set, such as the one reported by Stevens *et al.* [67], is consistent with results from another study on multicomponent sorption calculations with the DMS model [110], according to which the most accurate multicomponent predictions are *not* obtained with the best-fit parameter set regressed over one single sorption isotherm. In the same study [110], different parametrization schemes were tested for the prediction of CO_2/CH_4 sorption isotherms in high free volume glassy polymers (PIM-1, TZ-PIM, PTMSP). When a temperature dependence was imposed during the regression, the resulting DMS parameter sets yielded slightly more accurate multicomponent predictions. This improvement was not consistently observed in all the cases examined, but it appeared in the majority. Therefore, if a large experimental data set comprising several gases and temperatures is available, and if it is possible to follow the parametrization scheme adopted by Stevens *et al.* [67], this path would seem preferable to an independent parameterization at each temperature, and the corresponding predictions of the DMS model could be regarded with higher confidence.

However, from the point of view of robustness and consistency, the NELF model is always an appropriate choice.

Values for the adjustable parameters of the NELF model for these systems are also available in the literature [93]. These parameter sets, reported in **Table S6** (SI) for ease of comparison, were tested with respect to mixed-gas sorption calculations, and the results were compared with those obtained with the parameters optimized in this work (**Figure S7,** SI**)**. Results obtained using the parameters obtained in this study were only slightly more accurate than the ones obtained with literature parameters. The average relative deviations between the curves are 5.7% in the case of CO_2 sorption in HAB-6FDA, 4.3% for CH_4 sorption in HAB-6FDA, 2.3 % for CO_2 sorption in TR450 and 6.7% for CH4 sorption in TR450. The differences are significantly smaller than in the case of the DMS model (**Figure S4** in the SI). Therefore, in the NELF model, the use of literature parameters obtained for a different sample could also provide a reliable first estimate of mixed-gas sorption.

4.2.2. Solubility-Selectivity

Multicomponent solubility-selectivity values were calculated using Eq. (4) with the measured mixed-gas sorption data, and they are compared in **Figure 5** with ideal solubility-selectivity values calculated from pure-gas sorption data reported in [67]. **Figure 5** also shows predictions made using the DMS and NELF models.

The multicomponent values differ significantly from the ideal values: they are up to 6 times higher, meaning that competitive sorption has a positive impact on separation performance, acting to enhance selectivity. Moreover, the mixed-gas solubility-selectivity under these conditions increases as total pressure increases, while the ideal values would suggest the opposite. The discrepancies between the multicomponent and ideal results for α^S emphasize the necessity of accounting for multicomponent effects when designing separation processes.

In the case of HAB-6FDA, both the DMS and the NELF model exhibit the same increasing trend with pressure shown in the experimental data, although NELF displays a weaker pressure dependence. The good representation of mixed-gas data yielded here by both models is also reflected in a closer agreement of solubility-selectivity data. However, while the same level of accuracy in the representation is obtained also in the case of TR450 for the NELF model, in this case the DMS model shows not only a weak quantitative agreement with the data, but also the opposite pressure dependence with respect to experimental data.

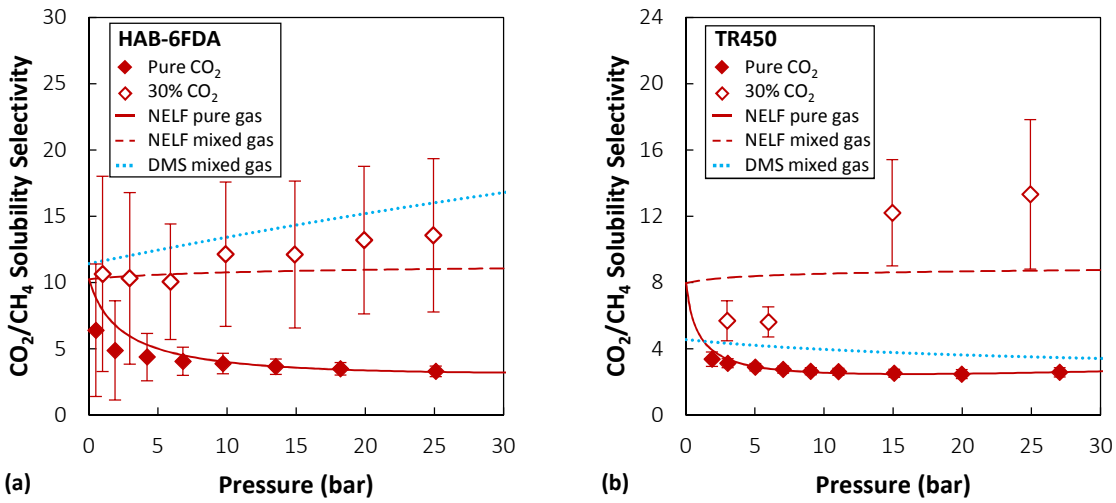

Figure 5. *Experimental solubility-selectivity for CO_2/CH_4 in HAB-6FDA (a) and TR450 (b). Empty diamonds represent multicomponent values, filled diamonds are ideal values calculated with pure-gas sorption data. Solid lines represent pure-gas results obtained with the NELF model. Dashed lines represent multicomponent calculations with the NELF model, the dotted ones are obtained with the multicomponent DMS model.*

Journal Pre-proof

Journal Pre-proof

5. The role of solubility-selectivity in multicomponent performance

5.1. Analysis of mixed-gas permeation data of HAB-6FDA and TR-450

Pure-gas measurements revealed that the main factor behind the higher permeability of TR polymers compared to their polyimide precursors is an order of magnitude increase in gas diffusivity. This result is consistent with the difference in fractional free volume between the materials analyzed, which increased from 15.0% to 19.6% following the thermal rearrangement process [66]. On the other hand, solubility increased by a factor of only ~2 after thermal rearrangement, providing a more modest contribution to the overall increase in permeability. The differences in gas solubility and diffusivity between HAB-6FDA and TR450 are proportionally higher for CH_4 than for CO_2, and TR450 therefore exhibits a lower permselectivity than that of HAB-6FDA [46,66].

Gleason *et al.* [20] measured the pure CO_2 and CH_4 permeability and mixed-gas permeability of a 50:50 CO_2/CH_4 mixture in HAB-6FDA and TR450 at 35 °C. From Eq. (2), with the permselectivity data reported from their work [20] and solubility-selectivity values calculated with the NELF model, the ideal diffusivity-selectivity of the two materials was computed, along with the multicomponent diffusivity-selectivity for a 50:50 mixture. The predictions of the NELF model were validated here against experimental data measured at a different gas mixture composition (30 mol% CO_2). Results from three different glassy polymer materials (PIM-1, TZ-PIM, PTMSP) [32], however, confirmed that the same parameter set yielded mixed-gas sorption predictions of the same accuracy for different gas compositions (10/30/50 mol% CO_2). Therefore, having validated the parameter set at one composition, it is reliable and highly beneficial time-wise to use the model to predict multicomponent sorption isotherms at another composition, rather than to measure them at every gas composition of interest.

In **Figure 6** the result of this separation of permselectivity into solubility and diffusivity selectivities is shown for the case of pure-gas measurements. Ideal (*i.e.*, pure-gas) permselectivity as a function of gas fugacity can be read on the *y*-axis as the total height of the bars. The ideal solubility-selectivity and ideal diffusivity-selectivity are also reported on the plot for each bar of the histogram, highlighting the contribution of each term to the overall permselectivity. Note that the ideal diffusivity-selectivity is the most relevant factor for both materials, and it is approximately 2 to 4 times higher than the ideal solubility-selectivity over the pressure range examined. Even though, in the pure gas case, the absolute value of α^D is slightly higher for HAB-6FDA (*i.e.*, 8.0 to 13.3 versus 8.0 to 8.8 for

TR450), it is the combination of high α^D and diffusion coefficients that places TR polymers near or beyond the diffusivity upper bound for CO_2/CH_4 [60].

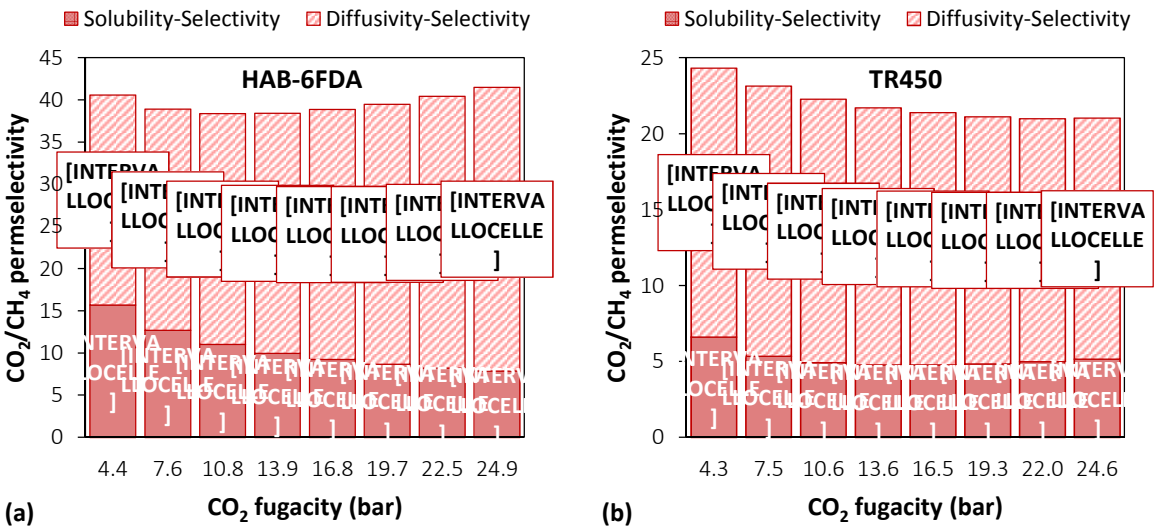

Figure 6. *Pure-gas CO_2/CH_4 permselectivity of (a) HAB-6FDA and (b) TR450 at 35 °C* [20] *split into its ideal solubility-selectivity and pure-gas diffusivity-selectivity components. α^S values were calculated using the NELF model, α^D values were calculated as the ratio of experimental permselectivity and calculated solubility-selectivity.*

Typically, in CO_2/CH_4 separation, CO_2 acts as a swelling agent, dilating the polymer matrix. When the CO_2 content of the mixture is increased, there is often a substantial concomitant decrease in permselectivity, as found in materials such as cellulose acetate and various polyimides [23,80,111–114]. In contrast, HAB-6FDA and TR450 show a slightly higher permselectivity in the mixed-gas test [20]. To analyze this interesting behavior, the same deconvolution into solubility- and diffusivity-selectivity was performed for the mixed-gas case, with results shown in **Figure 7**. Contrary to the pure-gas case, the biggest contribution to selectivity in the multicomponent case comes from sorption. The increase in solubility-selectivity outweighs the decrease in diffusivity-selectivity and is indeed responsible for the higher permselectivity observed during mixed-gas permeation experiments, confirming the hypothesis of Gleason *et al.* [20]. In the multicomponent case, the loss in diffusivity-selectivity is higher for the TR-polymer (from -58% at around 4 bar to -71% at about 22 bar), while the polyimide is capable of maintaining greater size sieving capability (*i.e.*, diffusivity-selectivity) in the multicomponent case, especially at low pressures (from -426% at around 4 bar to -69% at about 22 bar).

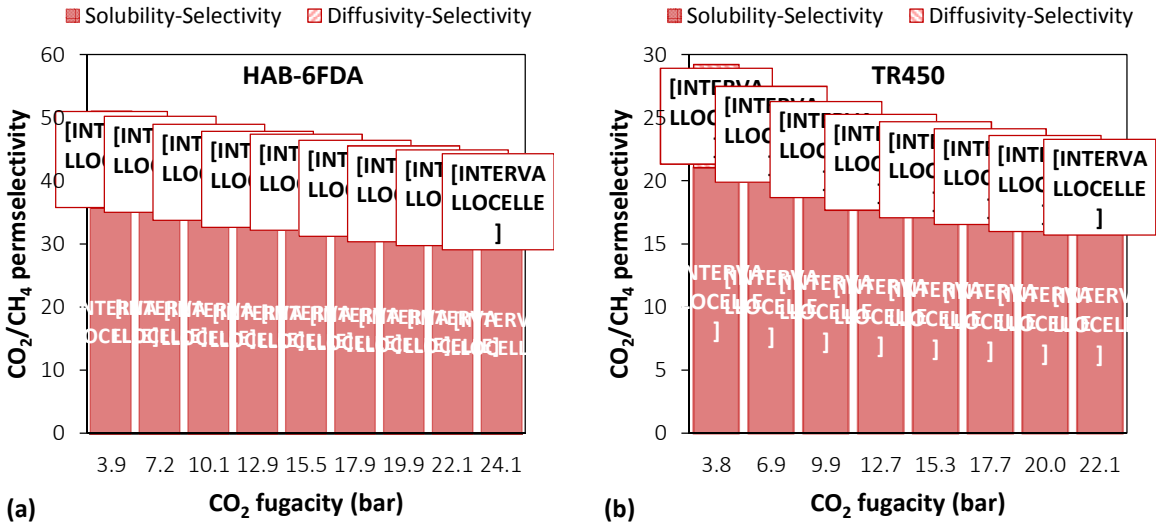

Figure 7. *Multicomponent CO_2/CH_4 permselectivity of (a) HAB-6FDA and (b) TR450 at 35 °C and 50 mol% CO_2 mixture composition* [20] *split into its solubility-selectivity and diffusivity-selectivity components. α^S values were calculated using the NELF model, α^D values were obtained as the ratio of experimental permselectivity and calculated solubility-selectivity.*

Plotting the ratio α^S/α^D as a function of CO_2 fugacity (**Figure 8**) allowed us to gather more information regarding the fundamental contributions of solubility and diffusivity to the mixed-gas permeability values reported by Gleason *et al.* [20]. As **Figure 8** indicates, the higher the fugacity, the more important is the contribution of solubility-selectivity over diffusivity-selectivity to the overall permselectivity, which decreases monotonically with increasing CO_2 fugacity (cf. **Figure 7**). TR450 has much higher values of α^S/α^D relative to the precursor polyimide, suggesting that the thermally rearranged polymer can more fully exploit the competitive sorption effect between CO_2 and CH_4.

Journal Pre-proof

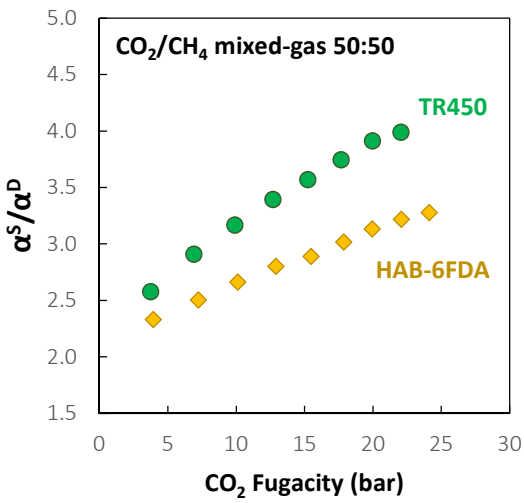

Figure 8. *Values of solubility-selectivity (predicted with NELF model) over diffusivity-selectivity (obtained by invoking the solution-diffusion model) as a function of CO_2 fugacity for HAB-6FDA (yellow diamonds) and TR450 (green circles) in the case of a 50:50 mixture of CO_2 and CH_4.*

5.2. Estimate of mixed-gas diffusion coefficients

We used the permeability data of Gleason *et al.* [20] together with NELF model calculations of solubility to estimate CO_2 and CH_4 diffusivities in HAB-6FDA and TR450 at 35 °C, at pure and multicomponent conditions (50:50 CO_2/CH_4), based on the solution-diffusion model (Eq. (2)). The results are shown in **Figure 9**, where pure-gas trends, represented with solid lines, can be compared with the independent results of Sanders *et al.* [66] obtained using the time-lag method. Even though data from different sources are involved in the comparison, the agreement between the directly measured diffusivities (square symbols in **Figure 9**) and the solution-diffusion calculation results is remarkable.

The same analysis repeated in the multicomponent case indicates that CH_4 diffusivity increases strongly in the presence of CO_2. This is a consequence of the CO_2-induced swelling of the polymer matrix, which, given the limited ability of CH_4 to dilate the material when it permeates alone, promotes faster diffusion of CH_4 in the multicomponent case than in the pure-gas case at the same fugacity. In fact, the increase in the CH_4 diffusion coefficient at multicomponent conditions relative to pure-gas conditions is stronger at higher fugacity, when swelling would be more pronounced, and grows from approximately 107% at 5 bar fugacity to 252% at 30 bar fugacity, in the case of the polyimide, and from 151% at 5 bar fugacity to 257% at 30 bar fugacity, in the case of TR450.

The same scenario also explains the very similar behavior observed for CO_2 in pure- and mixed-gas conditions. At the same CO_2 fugacity, CO_2 concentration inside the membrane barely changes in the multicomponent case relative to the pure-gas case, due to the limited

influence of competitive sorption by CH_4 on CO_2. Therefore, its swelling effect is comparable at pure- and mixed-gas conditions. However, when CO_2 fugacity is fixed, the presence of CH_4 in the multicomponent case can influence the diffusion paths available, even though it does not affect the equilibrium solubility. In the case of the polyimide, which is characterized by a lower free volume, the decrease in CO_2 diffusivity could be ascribed to competition among the diffusing gases for the available free volume. On the other hand, for TR450, the higher free volume available makes this effect less relevant, resulting in CO_2 diffusion coefficients that nearly overlap in pure and multicomponent conditions, as shown in **Figure 9**.

For direct comparison, **Figure 10** reports ideal and multicomponent values of α^D for the two materials. The depression of multicomponent diffusivity-selectivity shown in **Figure 10** compares well with that measured by other authors in different materials [22,33,42]. In particular, Garrido *et al.* [42] determined that, for a ~50 mol% CO_2/CH_4 mixture at ~2.2 bar partial pressure of CO_2, α^D in 6FDA-TMPDA decreased from a value of ~4 in pure-gas experiments to ~2 in mixed-gas conditions (51 mol% CO_2). Similar results reported by Fraga *et al.* [22] measured a CO_2/CH_4 multicomponent diffusivity-selectivity value in PIM-EA-TB of ~2 over a wide range of compositions (10-50 mol% CO_2), significantly lower than the value of ~4 determined by Carta *et al.* [43] from single-gas experiments.

Recently, a significant increase in CH_4 diffusivity at mixed-gas conditions (estimated through the solution-diffusion relation, like in the present study) was reported in the case of an equimolar CO_2/CH_4 mixture in PIM-Trip-TB [33] and 6FDA-mPDA [28]. In both cases, this was accompanied by an almost invariant CO_2 diffusivity. In the case of the higher free volume material PIM-Trip-TB, the estimated diffusivity-selectivity in multicomponent conditions ranged from ~2 to ~1.5, much lower than the value of ~5 obtained for the polyimide 6FDA-mPDA, which agrees quantitatively with the trend displayed here by HAB-6FDA and TR450.

Journal Pre-proof

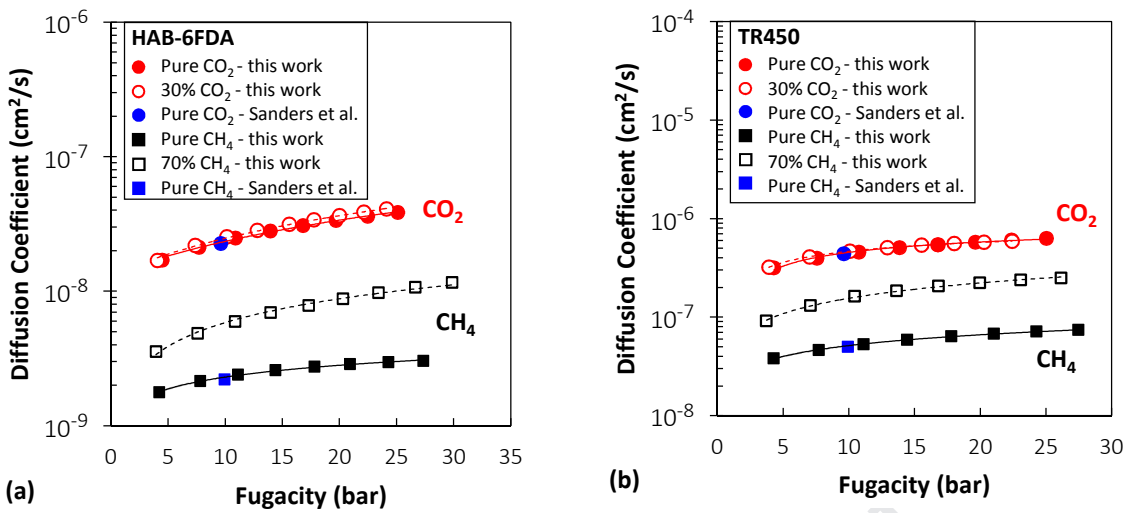

***Figure 9**. Diffusion coefficients of CO_2 (red) and CH_4 (black) calculated as detailed in Section 5.2 in the pure-gas case (solid lines) and in the case of a 50:50 mixture of the two gases (dashed lines) in (a) HAB-6FDA and (b) TR450 at 35 °C. Blue symbols are pure-gas values from ref.* [66] *reported for comparison.*

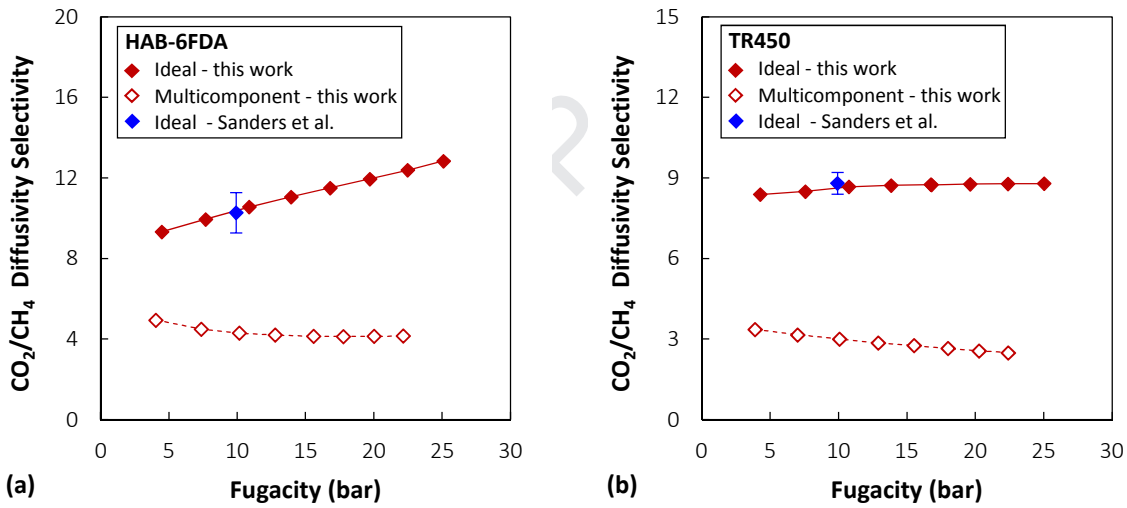

***Figure 10**. CO_2/CH_4 diffusivity-selectivity of (a) HAB-6FDA and (b) TR450 at 35 °C calculated as detailed in Section 5.1 in the pure-gas case (filled symbols and solid line) and in the multicomponent case (empty symbols and dashed line) for a 50:50 mixture (dashed lines). Blue symbols are pure-gas values from ref.* [66] *reported for comparison.*

5.3. Comparison with other glassy polymers

The solubility-selectivity and diffusivity-selectivity in pure-gas and mixed-gas conditions are compared for several polymeric membrane materials in **Figure 11**. A summary of the sources of the experimental data and the conditions under which they were obtained is given in **Table 5**. Note that, in order to obtain the selectivity values shown in **Figure 11**, **Figure 12** and **Figure 13**, the values of permeability, diffusivity and solubility were collected, for the same material, from different literature sources. Therefore, they refer to samples of the same

polymer with similar, but not identical, preparation protocols and history. Samples of the same material obtained in different studies can display slightly different gas transport properties, but despite some limited quantitative uncertainty due to combining data from different sources, the qualitative trends emerging from the present analysis are consistent and meaningful.

In the case of ultrahigh free volume glassy polymers, such as PIMs, the sorption factor plays a more significant role in ideal selectivity, so they are located closer to the parity-line than are materials like HAB-6FDA and TR450. Sometimes, as in the case of PIM-1 and cellulose triacetate (CTA), the ideal solubility-selectivity is even larger than the ideal diffusivity-selectivity [43,115,116], which is typical of behavior observed for rubbery materials, such as PDMS [34]. Mixed-gas experiments showed that solubility-selectivity increases relative to pure-gas solubility selectivity, presumably due to competitive sorption favoring solubility of CO_2 under mixed-gas conditions [32]. On the other hand, mixed-gas diffusivity-selectivity is always lower than pure-gas diffusivity-selectivity, as shown in **Figure 11** and, even more clearly, in **Figure 12**, where multicomponent permselectivity, solubility- and diffusivity-selectivity are compared to their analogous pure-gas values. This behavior is displayed by polymers belonging to very different categories (*i.e.*, PIMs, polyimides, TR polymers and cellulose acetate), and in particular, it is common also to materials that, based on pure-gas data, would be considered predominantly diffusivity-selective, like HAB-6FDA and TR450.

Concerning performance metrics, such as positioning with respect to the Robeson upper-bound at mixed-gas conditions, the same behavior was observed in all materials for which the contributions of multicomponent sorption and diffusion were isolated. Solubility-selectivity plays a decisive role in multicomponent permeability selectivity, while higher diffusivity is responsible for superior permeability, as reported in **Figure 11**. For instance, in the case of PIMs, their solubility-selectivity alone brings them very close to the upper bound.

Robeson *et al.* [60] analyzed the transport properties of TR polymers and PIMs relative to the upper bound and identified the importance of high solubility (compared to other materials) rather than high solubility-selectivity in shaping the exceptional performance of these families of materials. Although the current database for mixed-gas sorption is quite limited, the available evidence tends to support their conclusion that competitive sorption affects different families of polymers in a similar way.

Journal Pre-proof

Table 5. *Experimental conditions and source for the data represented in* ***Figure 11***, ***Figure 12***, ***Figure 13***.

	Ideal case			Multicomponent case			
	Ref.	**T (°C)**	**P (bar)**	**Ref.**	**%CO_2**	**T (°C)**	**P (bar)**
PIM-1	[25,115]	35	10	[25]	50	35	10
TZ-PIM	[21,32]	35	10	[21,32]	50/80	35	-
PIM-EA-TB	[43]	35	1-7	[22,117]	30	35	1
AO-PIM	[25]	35	10	[25,118]	50	35	10
PIM-Trip-TB	[33]	35	3	[33]	44	35	3
HAB-6FDA	[46,66,67]	35	10	[20] This work	50	35	10
TR-450	[46,66,67]	35	10	[20] This work	50	35	10
Matrimid	[87,119,120]	35	2	[41,120]	55	35	2
6FDA-mPDA	[28]	35	24	[28]	44	35	24
6FDA-TADPO	[121]	35	10	[27]	50	35	10
PPO	[122]	35	10	[123]	50	35	10
CTA	[124,125]	35	10	[125,126]	43/50	35	12

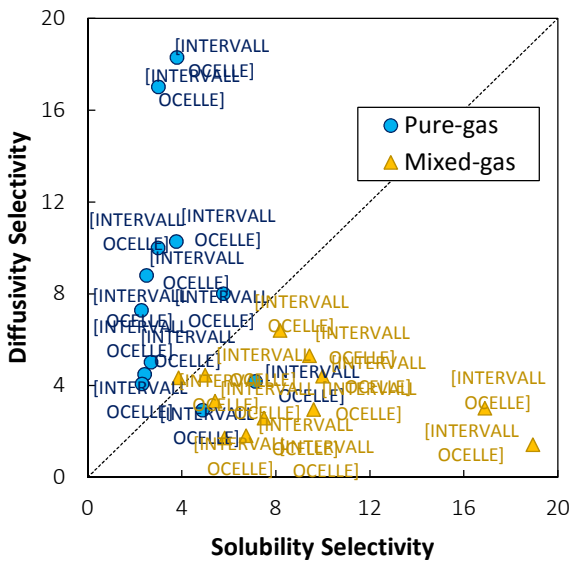

Figure 11. *Comparison of CO_2/CH_4 diffusivity- and solubility-selectivity in pure-gas and mixed-gas conditions for several polymeric materials. Sources of the experimental data and conditions of the tests are reported in* ***Table 5***.

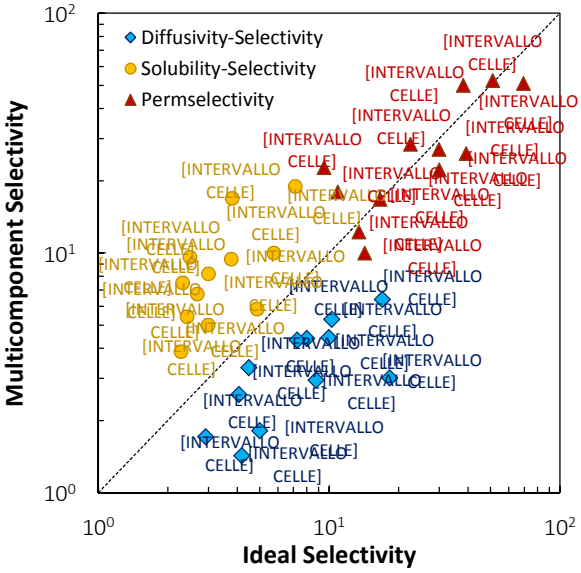

Figure 12. *Comparison of ideal (i.e., pure-gas) and multicomponent (i.e., mixed-gas) values of the CO_2/CH_4 permselectivity, diffusivity- and solubility-selectivity for several polymeric materials. Sources of the experimental data and conditions of the tests are reported in* ***Table 5****.*

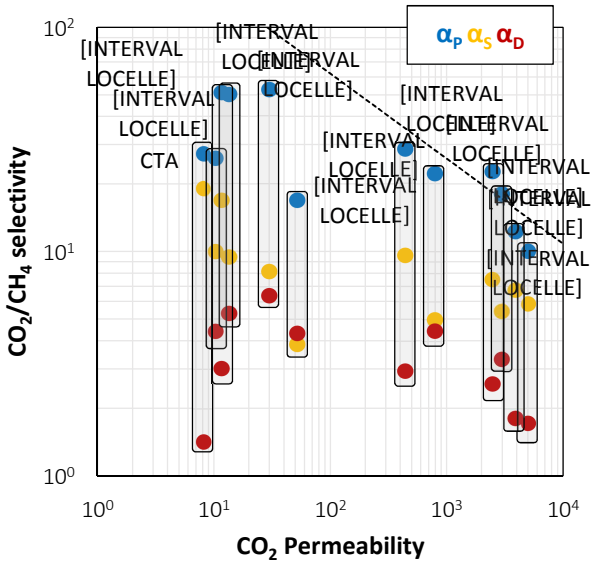

Figure 13. *CO_2/CH_4 Robeson upper bound and relative positioning of several materials in multicomponent conditions (sources and conditions of the tests are reported in* ***Table 5****). In the shaded column, solubility- and diffusivity-selectivity values are reported.*

6. Conclusions

In this study, multicomponent CO_2/CH_4 sorption was measured in HAB-6FDA polyimide and its thermally rearranged derivative, TR450, at 35 °C and ~30 mol% CO_2 mixture composition. The results of mixed-gas sorption experiments are consistent with those obtained for other glassy polymers and indicate that pronounced non-idealities due to competitive sorption are responsible for significant deviations of the multicomponent behavior from the pure-gas behavior.

Competitive sorption enhances the CO_2/CH_4 solubility-selectivity of glassy polymers: the less soluble gas (CH_4) experiences a significant exclusion effect (i.e., depression in solubility) when the other gas is present, while CO_2 sorption is barely affected by the presence of CH_4.

Modelling analysis of the mixed-gas sorption data was performed with the Non-Equilibrium Lattice Fluid model and the Dual Mode Sorption model. The results were validated against the mixed-gas measurements performed in this work.

It was possible to accurately predict multicomponent sorption with the NELF model using only pure-component parameters and binary parameters obtained from pure-gas sorption isotherms, and also with parameters already available in the literature. On the other hand, the accuracy of the DMS model calculations was strongly dependent on the method used to determine the model parameters, and the best results were obtained when a multi-temperature and multi-penetrant parameter fitting scheme was adopted. For both models, the mixture data were not used to obtain the model parameters, so multicomponent sorption can be calculated predictively if pure-gas sorption data are available. Since pure-gas measurements are widely accessible in the literature, a computationally inexpensive and reliable multicomponent model is a powerful tool for extracting additional and meaningful information from existing data.

A combined analysis of mixed-gas permeation and sorption data revealed that, when multicomponent effects are taken into account, the balance between the diffusivity and solubility factors is reversed, and the selectivity of the materials is solubility-driven. The presence of a swelling agent, such as CO_2, has a detrimental effect on the diffusivity-selectivity of the material, due to enhanced diffusion of CH_4 in the swollen polymer, and separation becomes controlled by solubility-selectivity. Nonetheless, high diffusivity values are key to achieving high permeability coefficients. Therefore, high free volume materials that allow for fast diffusion but are capable of achieving a more favorable sorption for the

faster components in a mixture are expected to exhibit higher permselectivity in multicomponent conditions.

References

[1] R.W. Baker, B.T. Low, Gas Separation Membrane Materials: A Perspective, Macomolecules. 47 (2014) 6999–7013. doi:10.1021/ma501488s.

[2] C. Li, S.M. Meckler, Z.P. Smith, J.E. Bachman, L. Maserati, J.R. Long, B.A. Helms, Engineered Transport in Microporous Materials and Membranes for Clean Energy Technologies, Adv. Mater. 30 (2018) 1704953. doi:10.1002/adma.201704953.

[3] W.J. Koros, C. Zhang, Materials for next-generation molecularly selective synthetic membranes, Nat. Mater. 16 (2017) 289–297. doi:10.1038/nmat4805.

[4] Y. He, F.M. Benedetti, S. Lin, C. Liu, Y. Zhao, H. Ye, T. Van Voorhis, M.G. De Angelis, T.M. Swager, Z.P. Smith, Polymers with Side Chain Porosity for Ultrapermeable and Plasticization Resistant Materials for Gas Separations, Adv. Mater. 31 (2019) 1807871. doi:10.1002/adma.201807871.

[5] H.W.H. Lai, F.M. Benedetti, Z. Jin, Y.C. Teo, A.X. Wu, M.G. De Angelis, Z.P. Smith, Y. Xia, Tuning the Molecular Weights, Chain Packing, and Gas-Transport Properties of CANAL Ladder Polymers by Short Alkyl Substitutions, Macromolecules. 52 (2019) 6294–6302. doi:10.1021/acs.macromol.9b01155.

[6] B.T. Low, Y. Wang, T. Chung, Polymeric Membranes for Energy Applications, Encycl. Polym. Sci. Technol. (2013) 1–37.

[7] S. Kim, Y.M. Lee, Rigid and microporous polymers for gas separation membranes, Prog. Polym. Sci. 43 (2015) 1–32. doi:10.1016/j.progpolymsci.2014.10.005.

[8] W. Kim, S. Nair, Membranes from nanoporous 1D and 2D materials: A review of opportunities, developments, and challenges, Chem. Eng. Sci. 104 (2013) 908–924. doi:10.1016/j.ces.2013.09.047.

[9] I. Rose, C.G. Bezzu, M. Carta, B. Comesaña-Gándara, E. Lasseuguette, M.C. Ferrari, P. Bernardo, G. Clarizia, A. Fuoco, J.C. Jansen, K.E. Hart, T.P. Liyana-Arachchi, C.M. Colina, N.B. McKeown, Polymer ultrapermeability from the inefficient packing of 2D chains, Nat. Mater. 16 (2017) 1–39. doi:10.1038/nmat4939.

[10] B.S. Ghanem, R. Swaidan, E. Litwiller, I. Pinnau, Ultra-microporous triptycene-based polyimide membranes for high-performance gas separation, Adv. Mater. 26 (2014) 3688–3692. doi:10.1002/adma.201306229.

[11] B.S. Ghanem, R. Swaidan, X. Ma, E. Litwiller, I. Pinnau, Energy-efficient hydrogen separation by AB-type ladder-polymer molecular sieves, Adv. Mater. 26 (2014) 6696–6700. doi:10.1002/adma.201401328.

[12] Y.C. Teo, H.W.H. Lai, Y. Xia, Synthesis of Ladder Polymers: Developments, Challenges, and Opportunities, Chem. - A Eur. J. 23 (2017) 14101–14112. doi:10.1002/chem.201702219.

[13] S. Luo, Q. Zhang, L. Zhu, H. Lin, B.A. Kazanowska, C.M. Doherty, A.J. Hill, P. Gao, R. Guo, Highly Selective and Permeable Microporous Polymer Membranes for Hydrogen Purification and CO2 Removal from Natural Gas, Chem. Mater. 30 (2018)

5322–5332. doi:10.1021/acs.chemmater.8b02102.

[14] R.W. Baker, K. Lokhandwala, Natural gas processing with membranes: An overview, Ind. Eng. Chem. Res. 47 (2008) 2109–2121. doi:10.1021/ie071083w.

[15] M. Galizia, W.S. Chi, Z.P. Smith, T.C. Merkel, R.W. Baker, B.D. Freeman, 50th Anniversary Perspective: Polymers and Mixed Matrix Membranes for Gas and Vapor Separation: A Review and Prospective Opportunities, Macromolecules. 50 (2017) 7809–7843. doi:10.1021/acs.macromol.7b01718.

[16] H.B. Park, J. Kamcev, L.M. Robeson, M. Elimelech, B.D. Freeman, Maximizing the right stuff: The trade-off between membrane permeability and selectivity, Science (80-.). 365 (2017) 1138–1148. doi:10.1126/science.aab0530.

[17] P. Luis, T. Van Gerven, B. Van Der Bruggen, Recent developments in membrane-based technologies for CO2 capture, Prog. Energy Combust. Sci. (2012). doi:10.1016/j.pecs.2012.01.004.

[18] G. George, N. Bhoria, S. Alhallaq, A. Abdala, V. Mittal, Polymer membranes for acid gas removal from natural gas, Sep. Purif. Technol. 158 (2016) 333–356. doi:10.1016/j.seppur.2015.12.033.

[19] J.G. Wijmans, R.W. Baker, The solution-diffusion model: a review, J. Memb. Sci. 107 (1995) 1–21. doi:10.1016/S0166-4115(08)60038-2.

[20] K.L. Gleason, Z.P. Smith, Q. Liu, D.R. Paul, B.D. Freeman, Pure- and mixed-gas permeation of CO2 and CH4 in thermally rearranged polymers based on 3,3′-dihydroxy-4,4′-diamino-biphenyl (HAB) and 2,2′-bis-(3,4-dicarboxyphenyl) hexafluoropropane dianhydride (6FDA), J. Memb. Sci. 475 (2015) 204–214. doi:10.1016/j.memsci.2014.10.014.

[21] N. Du, H.B. Park, G.P. Robertson, M.M. Dal-Cin, T. Visser, L. Scoles, M.D. Guiver, Polymer nanosieve membranes for CO2-capture applications, Nat. Mater. 10 (2011) 372–375. doi:10.1038/nmat2989.

[22] S.C. Fraga, M. Monteleone, M. Lanč, E. Esposito, A. Fuoco, L. Giorno, K. Pilnáček, K. Friess, M. Carta, N.B. McKeown, P. Izák, Z. Petrusová, J.G. Crespo, C. Brazinha, J.C. Jansen, A novel time lag method for the analysis of mixed gas diffusion in polymeric membranes by on-line mass spectrometry: Method development and validation, J. Memb. Sci. 561 (2018) 39–58. doi:10.1016/j.memsci.2018.04.029.

[23] M.D. Donohue, B.S. Minhas, S.Y. Lee, Permeation behavior of carbon dioxide-methane mixtures in cellulose acetate membranes, J. Memb. Sci. 42 (1989) 197–214. doi:10.1016/S0376-7388(00)82376-5.

[24] S. Basu, A. Cano-Odena, I.F.J. Vankelecom, MOF-containing mixed-matrix membranes for CO2/CH4 and CO2/N2 binary gas mixture separations, Sep. Purif. Technol. 81 (2011) 31–40. doi:10.1016/j.seppur.2011.06.037.

[25] R. Swaidan, B.S. Ghanem, E. Litwiller, I. Pinnau, Pure- and mixed-gas CO2/CH4 separation properties of PIM-1 and an amidoxime-functionalized PIM-1, J. Memb. Sci. 457 (2014) 95–102. doi:10.1016/j.memsci.2014.01.055.

[26] J.D. Wind, D.R. Paul, W.J. Koros, Natural gas permeation in polyimide membranes, J. Memb. Sci. 228 (2004) 227–236. doi:10.1016/j.memsci.2003.10.011.

Journal Pre-proof

[27] H.D. Kamaruddin, W.J. Koros, Some observations about the application of Fick's first law for membrane separation of multicomponent mixtures, J. Memb. Sci. 135 (1997) 147–159. doi:10.1016/S0376-7388(97)00142-7.

[28] G. Genduso, B.S. Ghanem, I. Pinnau, Experimental Mixed-Gas Permeability, Sorption and Diffusion of CO2-CH4 Mixtures in 6FDA-mPDA Polyimide Membrane: Unveiling the Effect of Competitive Sorption on Permeability Selectivity, Membranes (Basel). 9 (2019) 10. doi:10.3390/membranes9010010.

[29] O. Vopička, M.G. De Angelis, G.C. Sarti, Mixed gas sorption in glassy polymeric membranes: I. CO2 /CH4 and n-C4/CH4 mixtures sorption in poly(1-trimethylsilyl-1-propyne) (PTMSP), J. Memb. Sci. 449 (2014) 97–108. doi:10.1016/j.memsci.2013.06.065.

[30] O. Vopička, M.G. De Angelis, N. Du, N. Li, M.D. Guiver, G.C. Sarti, Mixed gas sorption in glassy polymeric membranes: II. CO2/CH4 mixtures in a polymer of intrinsic microporosity (PIM-1), J. Memb. Sci. 459 (2014) 264–276. doi:10.1016/j.memsci.2014.02.003.

[31] A.E. Gemeda, M.G. De Angelis, N. Du, N. Li, M.D. Guiver, G.C. Sarti, Mixed gas sorption in glassy polymeric membranes. III. CO2/CH4 mixtures in a polymer of intrinsic microporosity (PIM-1): Effect of temperature, J. Memb. Sci. 524 (2017) 746–757. doi:10.1016/j.memsci.2016.11.053.

[32] E. Ricci, A.E. Gemeda, N. Du, N. Li, M.G. De Angelis, M.D. Guiver, G.C. Sarti, Sorption of CO2/CH4 mixtures in TZ-PIM, PIM-1 and PTMSP: Experimental data and NELF-model analysis of competitive sorption and selectivity in mixed gases, J. Memb. Sci. 585 (2019) 136–149. doi:10.1016/j.memsci.2019.05.026.

[33] G. Genduso, Y. Wang, B.S. Ghanem, I. Pinnau, Permeation, sorption, and diffusion of CO2-CH4 mixtures in polymers of intrinsic microporosity: The effect of intrachain rigidity on plasticization resistance, J. Memb. Sci. 584 (2019) 100–109. doi:10.1016/j.memsci.2019.05.014.

[34] G. Genduso, E. Litwiller, X. Ma, S. Zampini, I. Pinnau, Mixed-gas sorption in polymers via a new barometric test system: sorption and diffusion of CO2-CH4 mixtures in polydimethylsiloxane (PDMS), J. Memb. Sci. 577 (2019) 195–204. doi:10.1016/j.memsci.2019.01.046.

[35] E.S. Sanders, W.J. Koros, H.B. Hopfenberg, V.T. Stannett, Mixed gas sorption in glassy polymers: Equipment design considerations and preliminary results, J. Memb. Sci. 13 (1983) 161–174. doi:10.1016/S0376-7388(00)80159-3.

[36] E.S. Sanders, W.J. Koros, H.B. Hopfenberg, Stannett, Pure and Mixed Gas Sorption of Carbon Dioxide and Ethylene in Poly(Methyl Methacrylate), J. Memb. Sci. 18 (1984) 53–74.

[37] E.S. Sanders, W.J. Koros, Sorption of CO2, C2H4, N2O and their Binary Mixtures in Poly(methyl methacrylate), J. Polym. Sci. B. 188 (1986) 175–188. doi:10.1002/polb.1986.180240117.

[38] R.D. Raharjo, B.D. Freeman, D.R. Paul, G.C. Sarti, E.S. Sanders, Pure and mixed gas CH4 and n-C4H10 permeability and diffusivity in poly(dimethylsiloxane), Polymer (Guildf). 306 (2007) 75–92. doi:10.1016/j.memsci.2007.08.014.

Journal Pre-proof

[39] R.D. Raharjo, B.D. Freeman, E.S. Sanders, Pure and mixed gas CH4 and n-C4H10 sorption and dilation in poly (dimethylsiloxane), J. Memb. Sci. 292 (2007) 45–61. doi:10.1016/j.memsci.2007.01.012.

[40] C.P. Ribeiro, B.D. Freeman, Carbon dioxide/ethane mixed-gas sorption and dilation in a cross-linked poly(ethylene oxide) copolymer, Polymer (Guildf). 51 (2010) 1156–1168. doi:10.1016/j.polymer.2010.01.012.

[41] E. Ricci, M. Minelli, M.G. De Angelis, A multiscale approach to predict the mixed gas separation performance of glassy polymeric membranes for CO2 capture: the case of CO2/CH4 mixture in Matrimid®, J. Memb. Sci. 539 (2017) 88–100. doi:https://doi.org/10.1016/j.memsci.2017.05.068.

[42] L. Garrido, C. García, M. López-González, B. Comesaña-Gándara, Á.E. Lozano, J. Guzmán, Determination of Gas Transport Coefficients of Mixed Gases in 6FDA-TMPDA Polyimide by NMR Spectroscopy, Macromolecules. 50 (2017) 3590–3597. doi:10.1021/acs.macromol.7b00384.

[43] M. Carta, R. Malpass-Evans, M. Croad, Y. Rogan, J.C. Jansen, P. Bernardo, F. Bazzarelli, N.B. McKeown, An Efficient Polymer Molecular Sieve for Membrane Gas Separations, Science (80-.). 339 (2013) 303–307. doi:10.1126/science.1228032.

[44] M. Lanč, K. Pilnáček, C.R. Mason, P.M. Budd, Y. Rogan, R. Malpass-Evans, M. Carta, B.C. Gándara, N.B. McKeown, J.C. Jansen, O. Vopička, K. Friess, Gas sorption in polymers of intrinsic microporosity: The difference between solubility coefficients determined via time-lag and direct sorption experiments, J. Memb. Sci. 570–571 (2018) 522–536. doi:10.1016/J.MEMSCI.2018.10.048.

[45] K. Pilnáček, O. Vopička, M. Lanč, M. Dendisová, M. Zgažar, P.M. Budd, M. Carta, R. Malpass-Evans, N.B. McKeown, K. Friess, Aging of polymers of intrinsic microporosity tracked by methanol vapour permeation, J. Memb. Sci. 520 (2016) 895–906. doi:10.1016/j.memsci.2016.08.054.

[46] Z.P. Smith, D.F. Sanders, C.P. Ribeiro, R. Guo, B.D. Freeman, D.R. Paul, J.E. McGrath, S. Swinnea, Gas sorption and characterization of thermally rearranged polyimides based on 3,3'-dihydroxy-4,4'-diamino-biphenyl (HAB) and 2,2'-bis-(3,4-dicarboxyphenyl) hexafluoropropane dianhydride (6FDA), J. Memb. Sci. 415–416 (2012) 558–567. doi:10.1016/j.memsci.2012.05.050.

[47] D.F. Sanders, Z.P. Smith, R. Guo, L.M. Robeson, J.E. McGrath, D.R. Paul, B.D. Freeman, Energy-efficient polymeric gas separation membranes for a sustainable future: A review, Polym. (United Kingdom). 54 (2013) 4729–4761. doi:10.1016/j.polymer.2013.05.075.

[48] B.S. Ghanem, N.B. McKeown, P.M. Budd, J.D. Selbie, D. Fritsch, High-performance membranes from polyimides with intrinsic microporosity, Adv. Mater. 20 (2008) 2766–2771. doi:10.1002/adma.200702400.

[49] B.S. Ghanem, N.B. McKeown, P.M. Budd, N.M. Al-Harbi, D. Fritsch, K. Heinrich, L. Starannikova, A. Tokarev, Y. Yampolskii, Synthesis, characterization, and gas permeation properties of a novel group of polymers with intrinsic microporosity: PIM-polyimides, Macromolecules. 42 (2009) 7881–7888. doi:10.1021/ma901430q.

[50] H.B. Park, C.H. Jung, Y.M. Lee, A.J. Hill, S.J. Pas, Polymers with Cavities Tuned for Fast Selective Transport of Small Molecules and Ions, Science (80-.). 318 (2007)

254–258. doi:10.1126/science.1146744.

[51] H.B. Park, S.H. Han, C.H. Jung, Y.M. Lee, A.J. Hill, Thermally rearranged (TR) polymer membranes for CO2 separation, J. Memb. Sci. 359 (2010) 11–24. doi:10.1016/j.memsci.2009.09.037.

[52] S.H. Han, H.J. Kwon, K.Y. Kim, J.G. Seong, C.H. Park, S. Kim, C.M. Doherty, A.W. Thornton, A.J. Hill, a E. Lozano, K. a Berchtold, Y.M. Lee, Tuning microcavities in thermally rearranged polymer membranes for CO2 capture., Phys. Chem. Chem. Phys. 14 (2012) 4365–73. doi:10.1039/c2cp23729f.

[53] C. Aguilar-Lugo, C. Álvarez, Y.M. Lee, J.G. de la Campa, Á.E. Lozano, Thermally Rearranged Polybenzoxazoles Containing Bulky Adamantyl Groups from Ortho-Substituted Precursor Copolyimides, Macromolecules. 51 (2018) 1605–1619. doi:10.1021/acs.macromol.7b02460.

[54] C.A. Scholes, B.D. Freeman, Thermal rearranged poly(imide-co-ethylene glycol) membranes for gas separation, J. Memb. Sci. 563 (2018) 676–683. doi:10.1016/J.MEMSCI.2018.06.027.

[55] S. Luo, Q. Zhang, T.K. Bear, T.E. Curtis, R.K. Roeder, C.M. Doherty, A.J. Hill, R. Guo, Triptycene-containing poly(benzoxazole-co-imide) membranes with enhanced mechanical strength for high-performance gas separation, J. Memb. Sci. 551 (2018) 305–314. doi:10.1016/J.MEMSCI.2018.01.052.

[56] S.M. Meckler, J.E. Bachman, B.P. Robertson, C. Zhu, J.R. Long, B.A. Helms, Thermally Rearranged Polymer Membranes Containing Tröger's Base Units Have Exceptional Performance for Air Separations, Angew. Chemie - Int. Ed. 57 (2018) 4912–4916. doi:10.1002/anie.201800556.

[57] Q. Liu, D.R. Paul, B.D. Freeman, Gas permeation and mechanical properties of thermally rearranged (TR) copolyimides, Polym. (United Kingdom). 82 (2016) 378–391. doi:10.1016/j.polymer.2015.11.051.

[58] S. Li, H.J. Jo, S.H. Han, C.H. Park, S. Kim, P.M. Budd, Y.M. Lee, Mechanically robust thermally rearranged (TR) polymer membranes with spirobisindane for gas separation, J. Memb. Sci. 434 (2013) 137–147. doi:10.1016/j.memsci.2013.01.011.

[59] L.M. Robeson, The upper bound revisited, J. Memb. Sci. 320 (2008) 390–400. doi:10.1016/j.memsci.2008.04.030.

[60] L.M. Robeson, M.E. Dose, B.D. Freeman, D.R. Paul, Analysis of the transport properties of thermally rearranged (TR) polymers and polymers of intrinsic microporosity (PIM) relative to upper bound performance, J. Memb. Sci. 525 (2017) 18–24. doi:10.1016/j.memsci.2016.11.085.

[61] M. Calle, A.E. Lozano, Y.M. Lee, Formation of thermally rearranged (TR) polybenzoxazoles: Effect of synthesis routes and polymer form, Eur. Polym. J. 48 (2012) 1313–1322. doi:10.1016/j.eurpolymj.2012.04.007.

[62] Y. Jiang, F.T. Willmore, D. Sanders, Z.P. Smith, C.P. Ribeiro, C.M. Doherty, A. Thornton, A.J. Hill, B.D. Freeman, I.C. Sanchez, Cavity size, sorption and transport characteristics of thermally rearranged (TR) polymers, Polymer (Guildf). 52 (2011) 2244–2254. doi:10.1016/j.polymer.2011.02.035.

[63] A. Brunetti, M. Cersosimo, J.S. Kim, G. Dong, E. Fontananova, Y.M. Lee, E. Drioli,

G. Barbieri, Thermally rearranged mixed matrix membranes for CO2 separation: An aging study, Int. J. Greenh. Gas Control. 61 (2017) 16–26. doi:10.1016/j.ijggc.2017.03.024.

[64] C.A. Scholes, B.D. Freeman, S.E. Kentish, Water vapor permeability and competitive sorption in thermally rearranged (TR) membranes, J. Memb. Sci. 470 (2014) 132–137. doi:10.1016/j.memsci.2014.07.024.

[65] Z.P. Smith, G. Hernández, K.L. Gleason, A. Anand, C.M. Doherty, K. Konstas, C. Alvarez, A.J. Hill, A.E. Lozano, D.R. Paul, B.D. Freeman, Effect of polymer structure on gas transport properties of selected aromatic polyimides, polyamides and TR polymers, J. Memb. Sci. 493 (2015) 766–781. doi:10.1016/j.memsci.2015.06.032.

[66] D.F. Sanders, Z.P. Smith, C.P. Ribeiro, R. Guo, J.E. McGrath, D.R. Paul, B.D. Freeman, Gas permeability, diffusivity, and free volume of thermally rearranged polymers based on 3,3′-dihydroxy-4,4′-diamino-biphenyl (HAB) and 2,2′-bis-(3,4-dicarboxyphenyl) hexafluoropropane dianhydride (6FDA), J. Memb. Sci. 409 (2012) 232–241. doi:10.1016/j.memsci.2012.03.060.

[67] K.A. Stevens, Z.P. Smith, K.L. Gleason, M. Galizia, D.R. Paul, B.D. Freeman, Influence of temperature on gas solubility in thermally rearranged (TR) polymers, J. Memb. Sci. 533 (2017) 75–83. doi:10.1016/j.memsci.2017.03.005.

[68] P. Meares, The Diffusion of Gases Through Polyvinyl Acetate, J. Am. Chem. Soc. 76 (1954) 3416–3422. doi:10.1021/ja01642a015.

[69] P. Meares, The solubilities of gases in polyvinyl acetate, Trans. Faraday Soc. 54 (1957) 40–46.

[70] R.M. Barrer, J.A. Barrie, J. Slater, Sorption and Diffusion in Ethyl Cellulose. Part III. Comparison between Ethyl Cellulose and Rubber, J. Polym. Sci. XXVII (1958) 177–197.

[71] A.S. Michaels, W.R. Vieth, J.A. Barrie, Diffusion of gases in polyethylene terephthalate, J. Appl. Phys. 34 (1963) 13–20. doi:10.1063/1.1729054.

[72] W.R. Vieth, H.H. Alcalay, A.J. Frabetti, Solution of Gases in Oriented Poly(ethylene Terephthalate), J. Appl. Polym. Sci. 8 (1964) 2125–2138. doi:10.1002/app.1964.070080513.

[73] W.R. Vieth, P.M. Tam, A.S. Michaels, Dual sorption mechanisms in glassy polystyrene, J. Colloid Interface Sci. 22 (1966) 360–370. doi:10.1016/0021-9797(66)90016-6.

[74] W.R. Vieth, J.M. Howell, J.H. Hsieh, B. Engrneerrng, R. Unrverslty, N. Brunswzck, Dual sorption theory, J. Memb. Sci. 1 (1976) 177–220. doi:10.1016/S0376-7388(00)82267-X.

[75] W.J. Koros, D.R. Paul, A.A. Rocha, Carbon dioxide sorption and transport in polycarbonate., J. Polym. Sci. Polym. Phys. 14 (1976) 687–702. doi:10.1002/pol.1976.180140410.

[76] D.R. Paul, W.J. Koros, Effect of partially immobilizing sorption on permeability and the diffusion time lag., J. Polym. Sci. Polym. Phys. Ed. 14 (1976) 675–685. doi:10.1002/pol.1976.180140409.

Journal Pre-proof

[77] G.H. Fredrickson, E. Helfand, Dual-Mode Transport of Penetrants in Glassy Polymers, Macromolecules. 18 (1985) 2201–2207. doi:10.1021/ma00153a024.

[78] W.J. Koros, Model for sorption of mixed gases in glassy polymers, J. Polym. Sci. Polym. Phys. Ed. 18 (1980) 981–992. doi:10.1002/pol.1980.180180506.

[79] W.J. Koros, E.S. Sanders, Multicomponent gas sorption in glassy polymers, J. Polym. Sci. Polym. Symp. (1985) 141–149. doi:10.1002/polc.5070720119.

[80] B.J. Story, W.J. Koros, Sorption of CO2/CH4 mixtures in poly(phenylene oxide) and a carboxylated derivative, J. Appl. Polym. Sci. 42 (1991) 2613–2626. doi:10.1002/app.1991.070420926.

[81] F. Doghieri, G.C. Sarti, Nonequilibrium Lattice Fluids: A Predictive Model for the Solubility in Glassy Polymers, Macromolecules. 29 (1996) 7885–7896. doi:10.1021/ma951366c.

[82] G.C. Sarti, F. Doghieri, Predictions of the solubility of gases in glassy polymers based on the NELF model, Chem. Eng. Sci. 53 (1998) 3435–3447. doi:10.1016/S0009-2509(98)00143-2.

[83] F. Doghieri, G.C. Sarti, Predicting the low pressure solubility of gases and vapors in glassy polymers by the NELF model, J. Memb. Sci. 147 (1998) 73–86. doi:10.1016/S0376-7388(98)00123-9.

[84] F. Doghieri, M. Quinzi, D.G. Rethwisch, G.C. Sarti, Predicting Gas Solubility in Glassy Polymers through Nonequilibrium EOS, in: Adv. Mater. Membr. Sep., American Chemical Society, Washington, DC, USA, 2004: pp. 74–90. doi:10.1021/bk-2004-0876.ch005.

[85] M.G. De Angelis, G.C. Sarti, Solubility of Gases and Liquids in Glassy Polymers, Annu. Rev. Chem. Biomol. Eng. 2 (2011) 97–120. doi:10.1146/annurev-chembioeng-061010-114247.

[86] F. Doghieri, M. Minelli, C.J. Durning, S. Kumar, Non-equilibrium thermodynamics of glassy polymers: Use of equations of state to predict gas solubility and heat capacity, Fluid Phase Equilib. 417 (2016) 144–157. doi:10.1016/j.fluid.2016.02.022.

[87] M. Minelli, G. Cocchi, L. Ansaloni, M.G. Baschetti, M.G. De Angelis, F. Doghieri, Vapor and liquid sorption in matrimid polyimide: Experimental characterization and modeling, Ind. Eng. Chem. Res. 52 (2013) 8936–8945. doi:10.1021/ie3027873.

[88] F. Doghieri, M.G. De Angelis, M.G. Baschetti, G.C. Sarti, Solubility of gases and vapors in glassy polymers modelled through non-equilibrium PHSC theory, Fluid Phase Equilib. 241 (2006) 300–307. doi:10.1016/j.fluid.2005.12.040.

[89] M.G. De Angelis, G.C. Sarti, F. Doghieri, NELF model prediction of the infinite dilution gas solubility in glassy polymers, J. Memb. Sci. 289 (2007) 106–122. doi:10.1016/j.memsci.2006.11.044.

[90] M. Minelli, M.G.M.G. De Angelis, An equation of state (EoS) based model for the fluid solubility in semicrystalline polymers, Fluid Phase Equilib. 367 (2014) 173–181. doi:10.1016/j.fluid.2014.01.024.

[91] M.K. Ghosh, K.L. Mital, Polyimides: Fundamentals and applications, CRC press, 2018. doi:10.1201/9780203742945.

Journal Pre-proof

[92] H. Ohya, V. V. Kudryavsev, S. I., Polyimide membranes: applications, fabrications and properties, CRC Press, 1997.

[93] M. Galizia, K.A. Stevens, Z.P. Smith, D.R. Paul, B.D. Freeman, Nonequilibrium lattice fluid modeling of gas solubility in HAB-6FDA polyimide and its thermally rearranged analogues, Macromolecules. 49 (2016) 8768–8779. doi:10.1021/acs.macromol.6b01479.

[94] D. Peng, D.B. Robinson, A New Two-Constant Equation of State, Ind. Eng. Chem. Fundam. 15 (1976) 59–64. doi:10.1021/i160057a011.

[95] S.I. Sandler, Chemical, Biochemical, and Engineering Thermodynamics, 5th Editio, John Wiley & Sons, Hoboken, NJ, USA, 2017.

[96] I.C. Sanchez, R.H. Lacombe, An elementary molecular theory of classical fluids. Pure fluids, J. Phys. Chem. 80 (1976) 2352–2362. doi:10.1021/j100562a008.

[97] R.H. Lacombe, I.C. Sanchez, Statistical Thermodynamics of Fluid Mixtures, J. Phys. Chem. 80 (1976) 2568–2580. doi:10.1021/j100564a009.

[98] I.C. Sanchez, R.H. Lacombe, Statistical Thermodynamics of Polymer Solutions, Macomolecules. 11 (1978) 1145–1156. http://pubs.acs.org/doi/pdf/10.1021/ma60066a017 (accessed June 26, 2017).

[99] J.H. Hildebrand, J.M. Prausnitz, R.L. Scott, Regular and Related Solutions: the Solubility of Gases, Liquids and Solids, Van Nostrand Reinhold Co., 1970.

[100] S.S. Jordan, W.J. Koros, A Free Volume Distribution Model of Gas Sorption and Dilation in Glassy Polymers, Macromolecules. 28 (1995) 2228–2235. doi:10.1021/ma00111a017.

[101] G.K. Fleming, W.J. Koros, Dilation of Polymers by Sorption of Carbon Dioxide at Elevated Pressures. 1. Silicone Rubber and Unconditioned Polycarbonate, Macromolecules. 19 (1986) 2285–2291. doi:10.1021/ma00162a030.

[102] D.S. Pope, G.K. Fleming, W.J. Koros, Effect of various exposure histories on sorption and dilation in a family of polycarbonates, Macromolecules. 23 (1990) 2988–2994. doi:10.1021/ma00213a029.

[103] M.G. De Angelis, T.C. Merkel, V.I. Bondar, B.D. Freeman, F. Doghieri, G.C. Sarti, Gas sorption and dilation in poly(2,2-bistrifluoromethyl-4,5-difluoro-1,3-dioxole-co-tetrafluoroethylene): Comparison of experimental data with predictions of the nonequilibrium lactice fluid model, Macromolecules. 35 (2002) 1276–1288. doi:10.1021/ma0106090.

[104] P.R. Bevington, D.K. Robinson, Data Reduction and Error Analysis for the Physical Sciences, 3rd edn., McGraw-Hill, Boston, MA, USA, 2003. doi:10.1063/1.4823194.

[105] V.I. Bondar, Y. Kamiya, Y.P. Yampol'skii, On pressure dependence of the parameters of the dual-mode sorption model, J. Polym. Sci. Part B Polym. Phys. 34 (1996) 369–378. doi:10.1002/(SICI)1099-0488(19960130)34:2<369::AID-POLB18>3.0.CO;2-H.

[106] E.S. Sanders, High-pressure sorption of pure and mixed gases in glassy polymers, North Carolina State University, Raleigh, 1983.

[107] W.J. Koros, D.R. Paul, Sorption and transport of various gases in polycarbonate, J.

Journal Pre-proof

Memb. Sci. 2 (1977) 165–190.

[108] S. Liu, C. Zhao, J. Lv, P. Lv, Y. Zhang, Density Characteristics of the CO2 -CH4 Binary System: Experimental Data at 313-353 K and 3-18 MPa and Modeling from the PC-SAFT EoS, J. Chem. Eng. Data. 63 (2018) 4368–4380. doi:10.1021/acs.jced.8b00433.

[109] M. Minelli, S. Campagnoli, M.G. De Angelis, F. Doghieri, G.C. Sarti, Predictive model for the solubility of fluid mixtures in glassy polymers, Macromolecules. 44 (2011) 4852–4862. doi:10.1021/ma200602d.

[110] E. Ricci, M.G. De Angelis, Modelling Mixed Gas Sorption in Glassy Polymers for CO2 Removal: a Sensitivity Analysis of the Dual Mode Sorption Model, Membranes (Basel). 9, 8 (2019).

[111] J.D. Wind, C. Staudt-Bickel, D.R. Paul, W.J. Koros, The Effects of Crosslinking Chemistry on CO2 Plasticization of Polyimide Gas Separation Membranes, Ind. Eng. Chem. Res. 41 (2002) 6139–6148. doi:10.1021/ie0204639.

[112] A. Bos, I.G.M. Pünt, M. Wessling, H. Strathmann, Plasticization-resistant glassy polyimide membranes for CO2/CH4 separations, Sep. Purif. Technol. 14 (1998) 27–39. doi:10.1016/S1383-5866(98)00057-4.

[113] T.A. Barbari, W.J. Koros, D.R. Paul, Polymeric membranes based on bisphenol-A for gas separations, J. Memb. Sci. 42 (1989) 69–86. doi:10.1016/S0376-7388(00)82366-2.

[114] S.M. Jordan, W.J. Koros, G.K. Fleming, The effects of CO2 exposure on pure and mixed gas permeation behavior: comparison of glassy polycarbonate and silicone rubber, J. Memb. Sci. 30 (1987) 191–212. doi:10.1016/S0376-7388(00)81351-4.

[115] P.M. Budd, K.J. Msayib, C.E. Tattershall, B.S. Ghanem, K.J. Reynolds, N.B. McKeown, D. Fritsch, Gas separation membranes from polymers of intrinsic microporosity, J. Memb. Sci. 251 (2005) 263–269. doi:10.1016/j.memsci.2005.01.009.

[116] R. Srinivasan, S.R. Auvil, P.M. Burban, Elucidating the mechanism(s) of gas transport in poly[1-(trimethylsilyl)-1-propyne] (PTMSP) membranes, J. Memb. Sci. 86 (1994) 67–86. doi:10.1016/0376-7388(93)E0128-7.

[117] F.M. Benedetti, E. Ricci, M.G. De Angelis, M. Carta, N.B. McKeown, Sorption of CO2/CH4 and their mixtures in PIM-EA-TB, Prep. (n.d.).

[118] A.E. Gemeda, Polymeric Gas Separation Membranes: CO2/CH4 Mixed Gas Sorption in Glassy Polymers, University of Bologna, 2015.

[119] L. Ansaloni, M. Minelli, M. Giacinti Baschetti, G.C. Sarti, Effects of Thermal Treatment and Physical Aging on the Gas Transport Properties in Matrimid®, Oil Gas Sci. Technol. – Rev. d'IFP Energies Nouv. 70 (2015) 367–379. doi:10.2516/ogst/2013188.

[120] A. Bos, High Pressure CO2/CH4 Separation with Glassy Polymer Membranes (Aspects of CO2-induced plasticization), Ph.D. Thes, University of Twente, Netherlands, 1996.

[121] D.R.B. Walker, W.J. Koros, Transport characterization of a polypyrrolone for gas separations, J. Memb. Sci. 55 (1991) 99–117. doi:10.1016/S0376-7388(00)82329-7.

Journal Pre-proof

[122] Y. Maeda, D.R. Paul, Selective gas transport in miscible PPO-PS blends, Polymer (Guildf). 26 (1985) 2055–2063. doi:10.1016/0032-3861(85)90187-9.

[123] B.J. Story, W.J. Koros, Comparison of three models for permeation of CO2/CH4 mixtures in poly(phenylene oxide), J. Polym. Sci. Part B Polym. Phys. 27 (1989) 1927–1948. doi:10.1002/polb.1989.090270910.

[124] A.C. Puleo, D.R. Paul, S.S. Kelley, The Effect Of Degree Of Acetylation On Gas Sorption And Transport Behaviour In Cellulose Acetate, J. Memb. Sci. 47 (1989) 301–332.

[125] R. Swaidan, B. Ghanem, M. Al-Saeedi, E. Litwiller, I. Pinnau, Role of intrachain rigidity in the plasticization of intrinsically microporous triptycene-based polyimide membranes in mixed-Gas CO2/CH4 separations, Macromolecules. 47 (2014) 7453–7462. doi:10.1021/ma501798v.

[126] G. Genduso, I. Pinnau, Quantification of sorption, diffusion, and plasticization properties of cellulose triacetate films under mixed-gas CO2/CH4 environment, J. Memb. Sci. (2020). doi:10.1016/j.memsci.2020.118269.

Journal Pre-proof

Journal Pre-proof

Competitive sorption in CO_2/CH_4 separations: the case of HAB-6FDA polyimide and its TR derivative and a general analysis of its impact on the selectivity of glassy polymers at multicomponent conditions

Eleonora Ricci[1], *Francesco M. Benedetti*[1,§], *Michelle E. Dose*[2], *M. Grazia De Angelis*[1,*], *Benny D. Freeman*[2], *Donald R. Paul*[2]

[1]Department of Civil, Chemical, Environmental and Materials Engineering, Alma Mater Studiorum – University of Bologna, Italy

[2]John J. McKetta Jr. Department of Chemical Engineering – The University of Texas at Austin, United States

[§]**Present address:** Department of Chemical Engineering – Massachusetts Institute of Technology, United States

***Corresponding author:**
Maria Grazia De Angelis
grazia.deangelis@unibo.it

Tel. +39 (0) 51 2060410
Fax +39 (0) 51 6347788

Journal Pre-proof

– Highlights –

- Competitive sorption enhances CO_2/CH_4 solubility-selectivity in HAB-6FDA and TR450
- The NELF model predicts multicomponent sorption using only pure-gas data as input
- Solution-diffusion analysis was performed to extract mixed-gas diffusivities
- The multicomponent permselectivity of glassy polymers is driven by solubility

Journal Pre-proof

Declaration of interests

☒ The authors declare that they have no known competing financial interests or personal relationships that could have appeared to influence the work reported in this paper.

☐The authors declare the following financial interests/personal relationships which may be considered as potential competing interests:

Journal Pre-p